

Electronic Supporting Information

Ni(II) and Pd(II) complexes of a new redox-active pentadentate azo-appended 2-aminophenol ligand: Pd(II)-assisted intraligand cyclization forms phenoxazinyl ring

Saumitra Bhowmik, Arunava Sengupta and Rabindranath Mukherjee*

Figures:

Fig. S1 ^1H NMR (CDCl_3 , 500 MHz) spectrum of H_4L .

Fig. S2 ^{13}C NMR (CDCl_3 , 125 MHz) spectrum of H_4L .

Fig. S3 Positive-Ion ESI-MS spectrum of $\{\text{[H}_4\text{L] + H}^+\}$. The isotope distribution patterns of the molecular ion peaks shown in insets.

Fig. S4 Positive-Ion ESI-MS spectrum of $[\text{Ni(L)}]$ (**1**). The isotope distribution patterns of the molecular ion peaks shown in insets.

Fig. S5 Positive-Ion ESI-MS spectrum of $[\text{Pd(L)}]$ (**2**). The isotope distribution patterns of the molecular ion peaks shown in insets.

Fig. S6 Cyclic voltammogram (100 mV/s) of a 1.0 mM solution of $[\text{Ni(L)}]\text{SbF}_6 \bullet 2\text{CH}_2\text{Cl}_2$ (**3**• $2\text{CH}_2\text{Cl}_2$), in CH_2Cl_2 (0.1 M in TBAP) at a platinum working electrode.

Fig. S7 Positive-Ion ESI-MS spectrum of $[\text{Ni(L)}]\text{SbF}_6 \bullet 2\text{CH}_2\text{Cl}_2$ (**3**• $2\text{CH}_2\text{Cl}_2$).

Fig. S8 ^1H NMR spectra (500 MHz, CDCl_3) of complex **3**.

Fig. S9 X-band EPR spectra for **1** as solid recorded at (a) 300 K and (b) 80 K, along with their simulated versions.

Fig. S10 X-band EPR spectra for **2** as solid recorded at (a) 300 K and (b) 80 K, along with their simulated versions.

Fig. S11 Positive-Ion ESI-MS spectrum of $[\text{Pd(L}^*)]$ (**4**). The isotope distribution patterns of the molecular ion peaks shown in insets.

Fig. S12 X-band EPR spectra for **4** as solid recorded at (a) 300 K and (b) 80 K, along with their simulated versions.

Fig. S13 TD-DFT-calculated electronic spectrum for $[\text{Ni(L)}]$ (**1**).

Fig. S14 Representative molecular-orbitals involved in TD-DFT transitions for $[\text{Ni(L)}]$ (**1**).

Fig. S15 TD-DFT-calculated electronic spectrum for $[\text{Ni(L)}]\text{SbF}_6 \bullet 2\text{CH}_2\text{Cl}_2$ (**3**• $2\text{CH}_2\text{Cl}_2$).

Fig. S16 Representative molecular-orbitals involved in TD-DFT transitions for $[\text{Ni(L)}]-\text{SbF}_6 \bullet 2\text{CH}_2\text{Cl}_2$ (**3**• $2\text{CH}_2\text{Cl}_2$).

Fig. S17 TD-DFT-calculated electronic spectrum for $[\text{Pd(L)}]$ (**2**).

Fig. S18 Representative molecular-orbitals involved in TD-DFT transitions for $[\text{Pd(L)}]$ (**2**).

Fig. S19 TD-DFT-calculated electronic spectrum for $[\text{Pd(L}^*)]$ (**4**).

Fig. S20 Representative molecular-orbitals involved in TD-DFT transitions for $[\text{Pd(L}^*)]$ (**4**).

Tables:

Table S1 Data collection and structure refinement parameters for $[\text{Ni(L)}]$ (**1**), $[\text{Pd(L)}]$ (**2**), $[\text{Ni(L)}]\text{SbF}_6 \bullet 2\text{CH}_2\text{Cl}_2$ (**3**• $2\text{CH}_2\text{Cl}_2$) and $[\text{Pd(L}^*)]$ (**4**).

Table S2 Bond angles for $[\text{Ni(L)}]$ (**1**), $[\text{Pd(L)}]$ (**2**), $[\text{Ni(L)}]\text{SbF}_6 \bullet 2\text{CH}_2\text{Cl}_2$ (**3**• $2\text{CH}_2\text{Cl}_2$) and $[\text{Pd(L}^*)]$ (**4**).

Table S3 X-ray Structural and DFT-Optimized Bond Lengths of **1–4**.

Table S4 Geometry-optimised cartesian coordinates for [Ni(L)] (**1**).

Table S5 Geometry-optimised cartesian coordinates for [Ni(L)]SbF₆•2CH₂Cl₂ (**3**•2CH₂Cl₂).

Table S6 Geometry-optimised cartesian coordinates for [Pd(L)] (**2**).

Table S7 Geometry-optimised cartesian coordinates for [Pd(L^{*})] (**4**).

Table S8 TD-DFT-calculated absorption spectral result for [Ni(L)] (**1**).

Table S9 TD-DFT-calculated absorption spectral result for [Ni(L)]SbF₆•CH₂Cl₂ (**3**•2CH₂Cl₂).

Table S10 TD-DFT-calculated absorption spectral result for [Pd(L)] (**2**).

Table S11 TD-DFT-calculated absorption spectral result for [Pd(L^{*})] (**4**).

Scheme S1 Explanation for metal ion azo bond switchover.

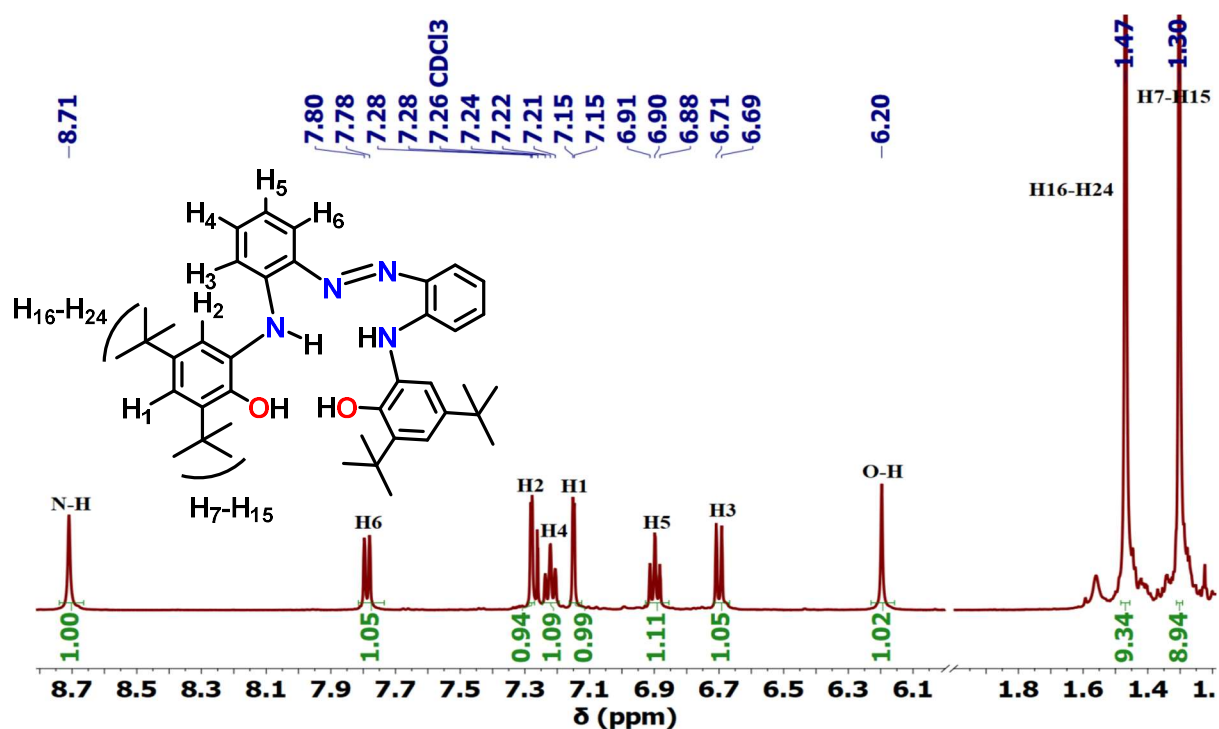


Fig. S1 ^1H NMR (CDCl_3 , 500 MHz) spectrum of H₄L .

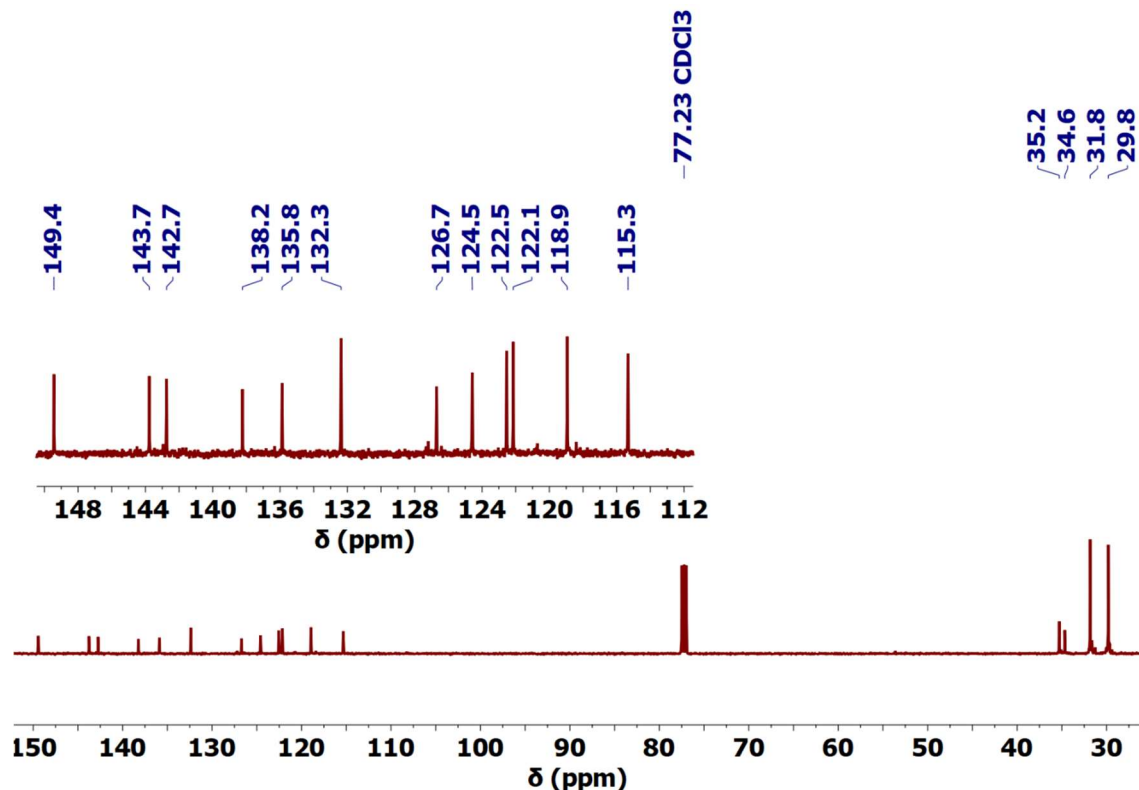


Fig. S2 ^{13}C NMR (CDCl_3 , 125 MHz) spectrum of H₄L.

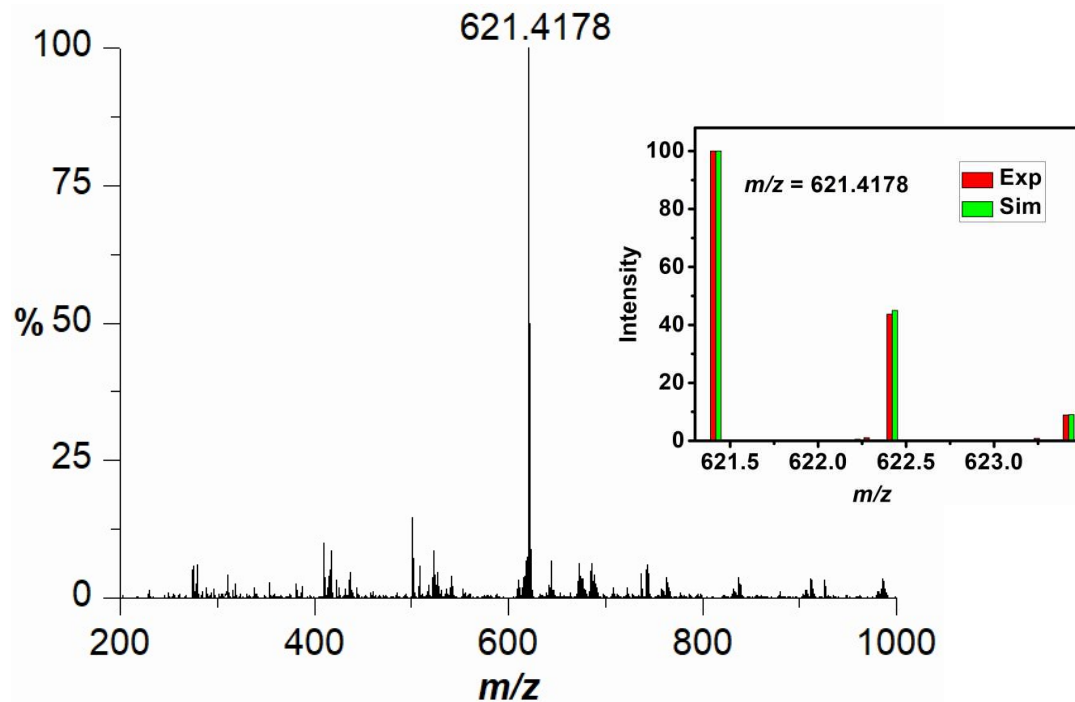


Fig. S3 Positive-Ion ESI-MS spectrum of $\{[\text{H}_4\text{L}] + \text{H}^+\}$. The isotope distribution patterns of the molecular ion peaks shown in insets.

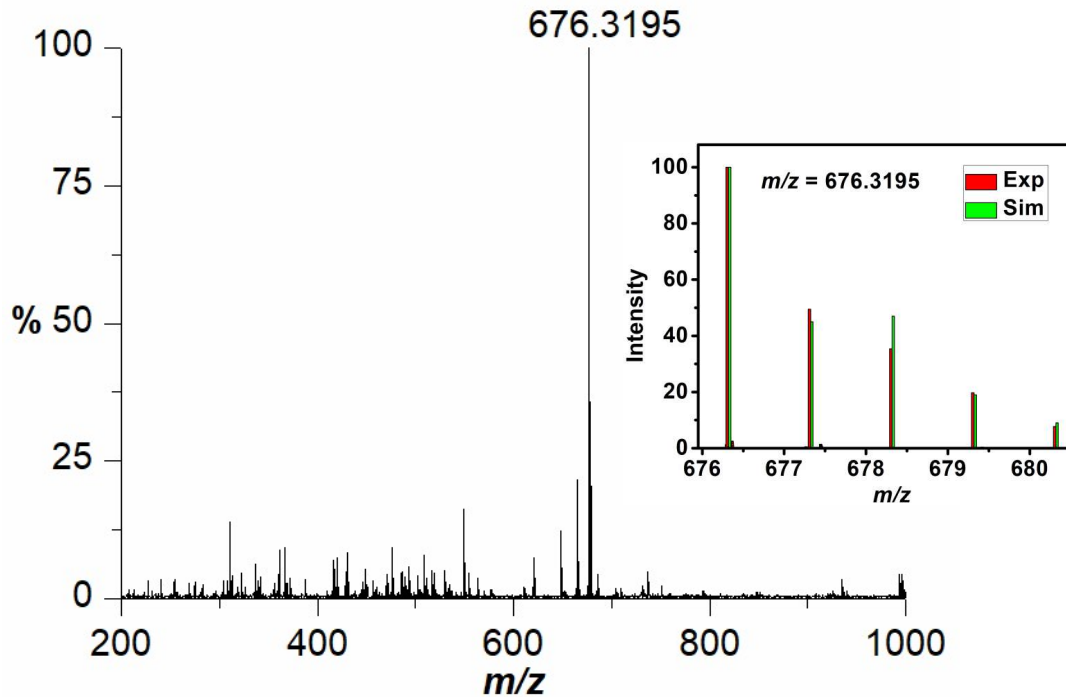


Fig. S4 Positive-Ion ESI-MS spectrum of $[\text{Ni}(\text{L})]$ (**1**): $\{[\text{Ni}(\text{L})] + \text{H}^+\}$. The isotope distribution patterns of the molecular ion peaks shown in insets.

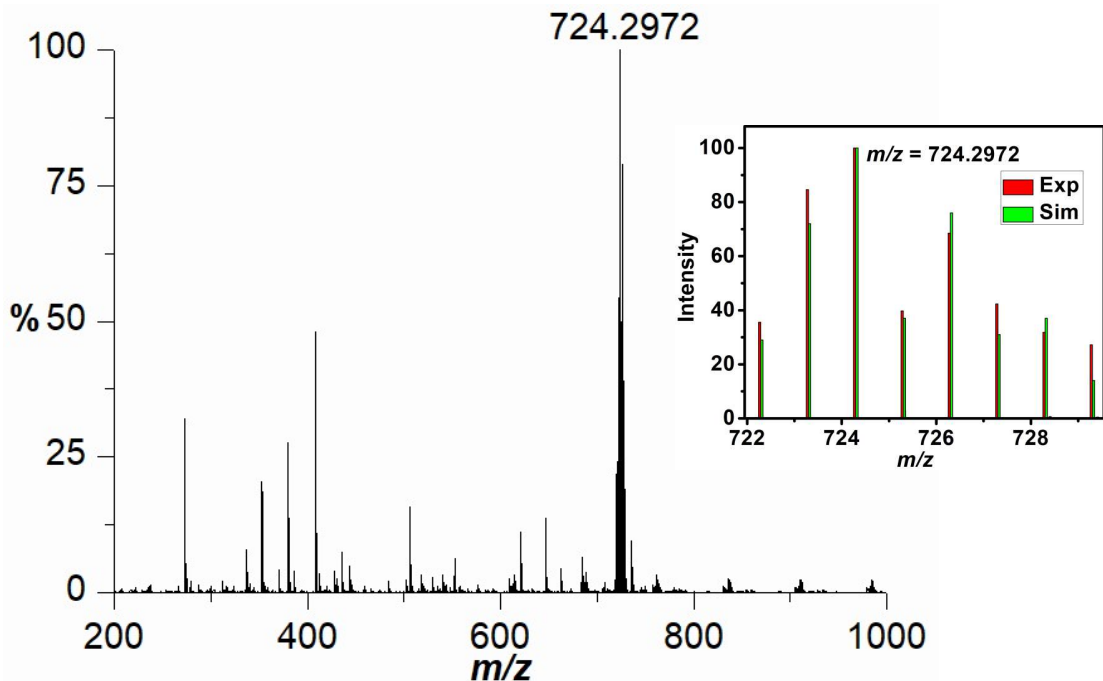


Fig. S5 Positive-Ion ESI-MS spectrum of $[\text{Pd}(\text{L})]$ (**2**): $\{[\text{Pd}(\text{L})]\} + \text{H}^+$. The isotope distribution patterns of the molecular ion peaks shown in insets.

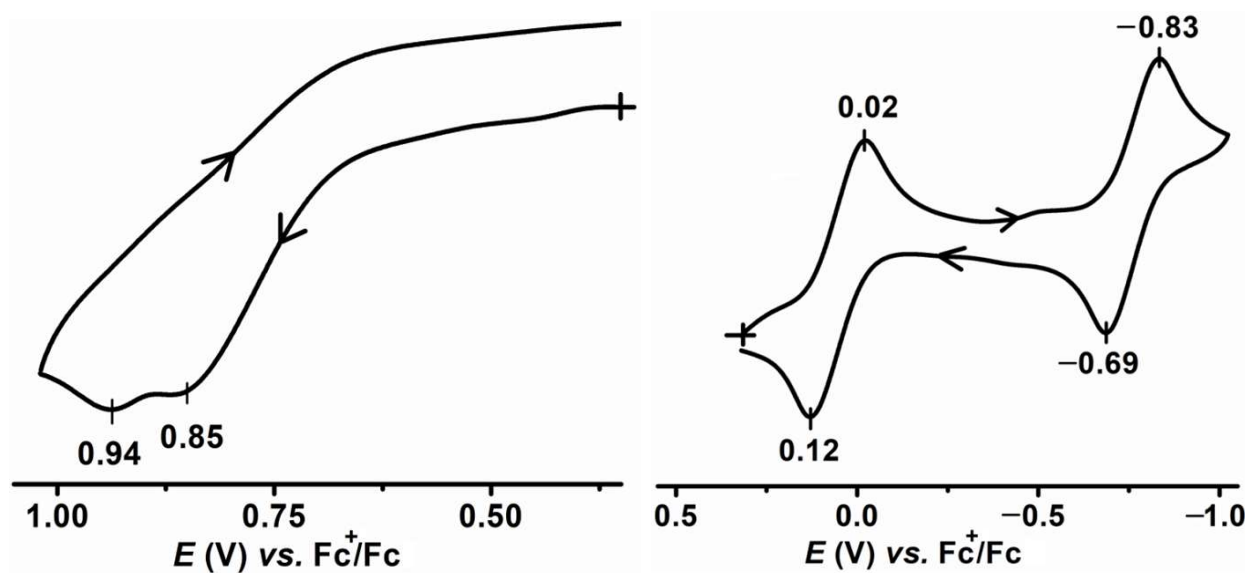


Fig. S6 Cyclic voltammogram (100 mV/s) of a 1.0 mM solution of $[\text{Ni}(\text{L})]\text{SbF}_6 \cdot 2\text{CH}_2\text{Cl}_2$ (**3**• $2\text{CH}_2\text{Cl}_2$), in CH_2Cl_2 (0.1 M in TBAP) at a platinum working electrode.

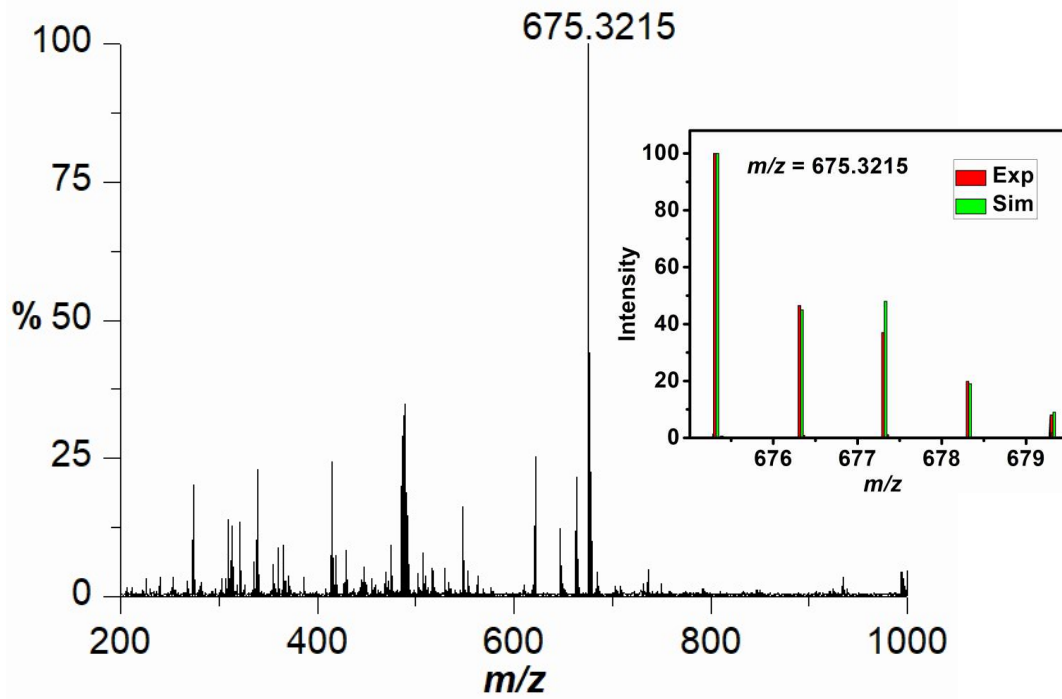


Fig. S7 Positive-Ion ESI-MS spectrum of $[\text{Ni}(\text{L})](\text{SbF}_6) \cdot 2\text{CH}_2\text{Cl}_2$ (**3**• $2\text{CH}_2\text{Cl}_2$): $\{[\text{Ni}(\text{L})]^+\}$. The isotope distribution patterns of the molecular ion peaks shown in insets.

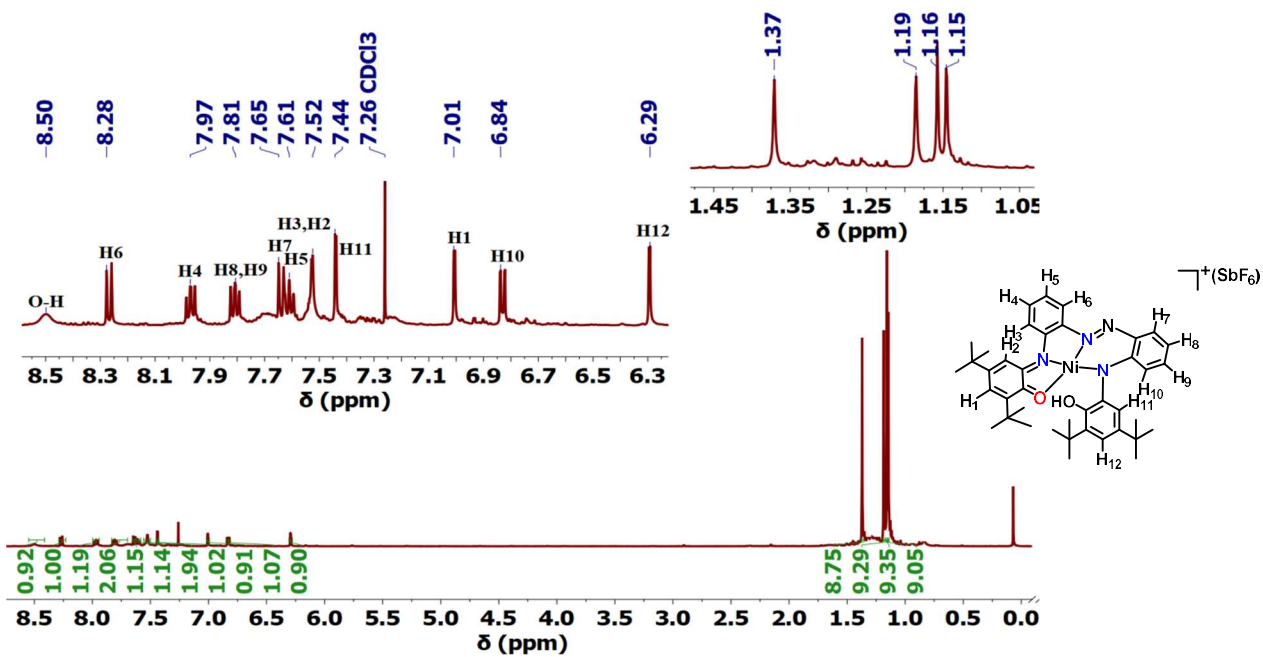
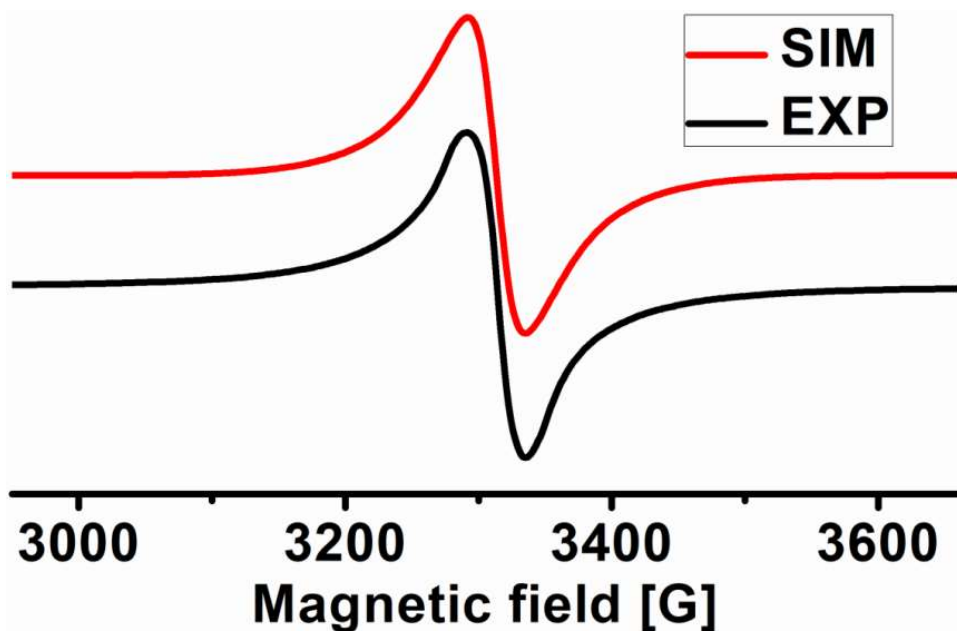


Fig. S8 ^1H NMR spectra (500 MHz, CDCl_3) of complex 3.

(a)



(b)

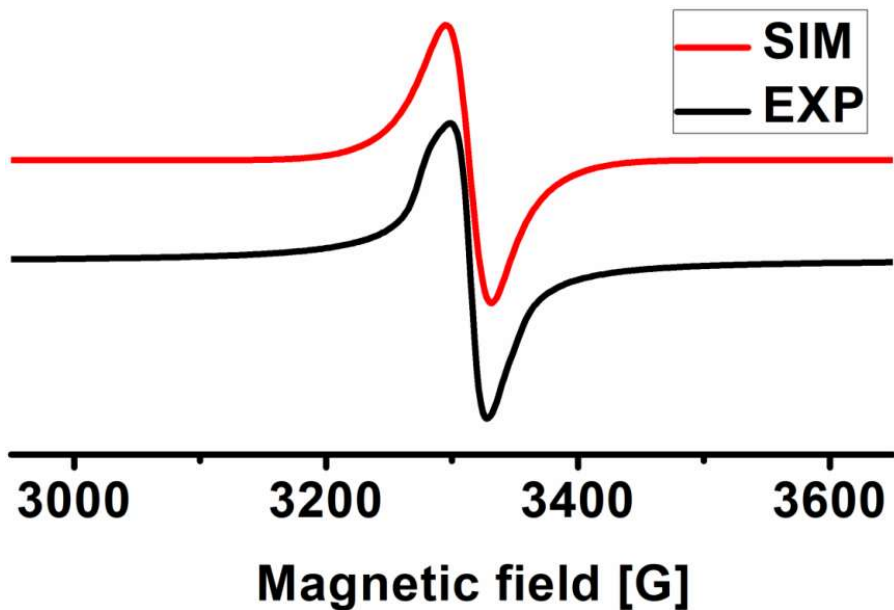
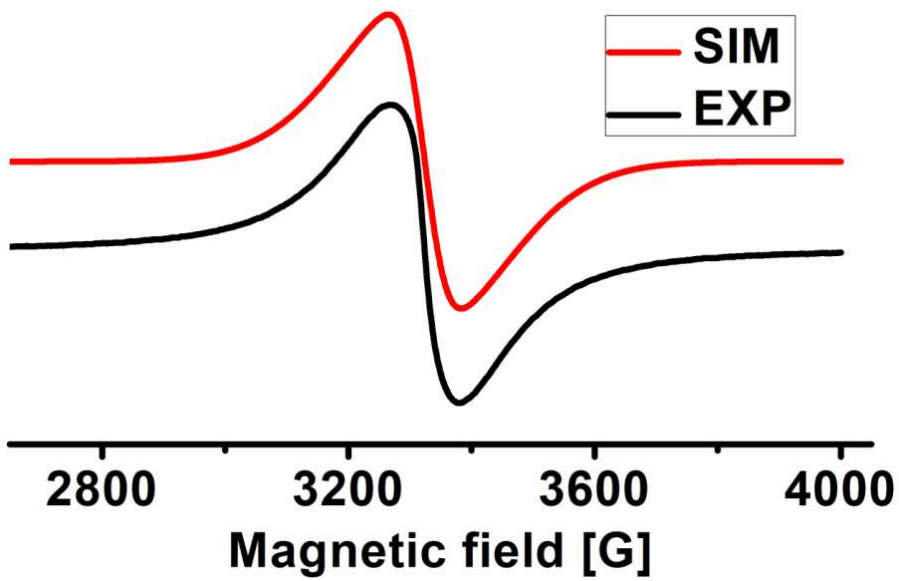


Fig. S9 X-band EPR spectrum ($\nu = 9.460$ GHz, power = 0.201 mW, receiver gain = 1×10^2 , modulation frequency = 100 KHz, modulation amplitude = 5.00 G) for **1** as solid recorded (a) as solid at 298 K, upper trace: simulated parameters: $g_x = g_y = g_z = 2.0075$; $W_x = 60$ G, $W_y = 185$ G, $W_z = 20$ G; (b) as solid at 80 K, simulated parameters: $g_x = g_y = g_z = 2.00757$; $W_x = 35$ G, $W_y = 115$ G, $W_z = 20$ G. Error limits: $g \pm 0.002$; $A \pm 0.0001$ cm $^{-1}$; $W \pm 1$.

(a)



(b)

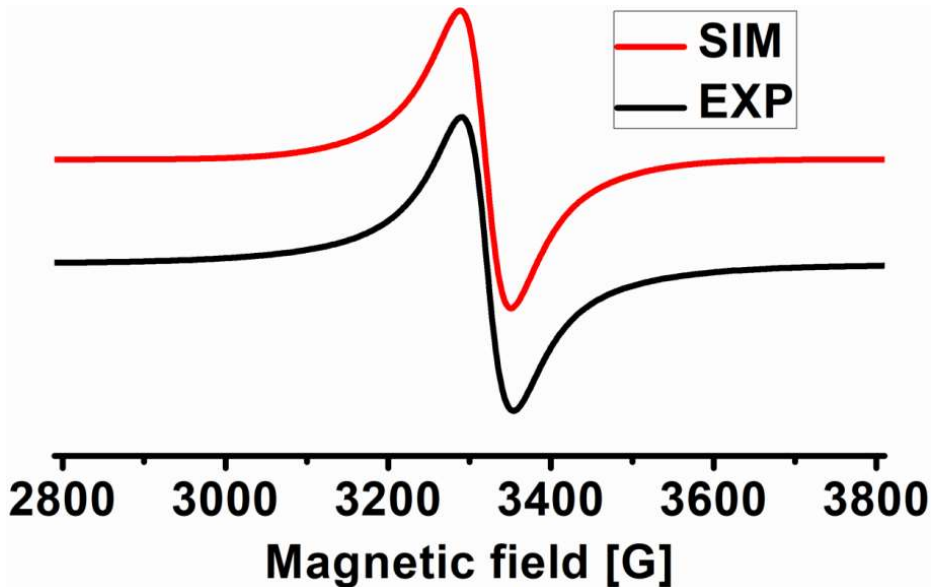


Fig. S10 X-band EPR spectrum ($\nu = 9.460$ GHz, power = 0.201 mW, receiver gain = 1×10^2 , modulation frequency = 100 KHz, modulation amplitude = 5.00 G) for **2** as solid recorded at (a) as solid at 298 K, upper trace: simulated parameters: $g_x = g_y = g_z = 1.9988$; $W_x = 55$ G, $W_y = 225$ G, $W_z = 325$ G; (b) as solid at 80 K, upper trace: simulated parameters: $g_x = g_y = g_z = 2.00378$; $W_x = 30$ G, $W_y = 275$ G, $W_z = 75$ G. Error limits: $g \pm 0.002$; $A \pm 0.0001$ cm $^{-1}$; $W \pm 1$.

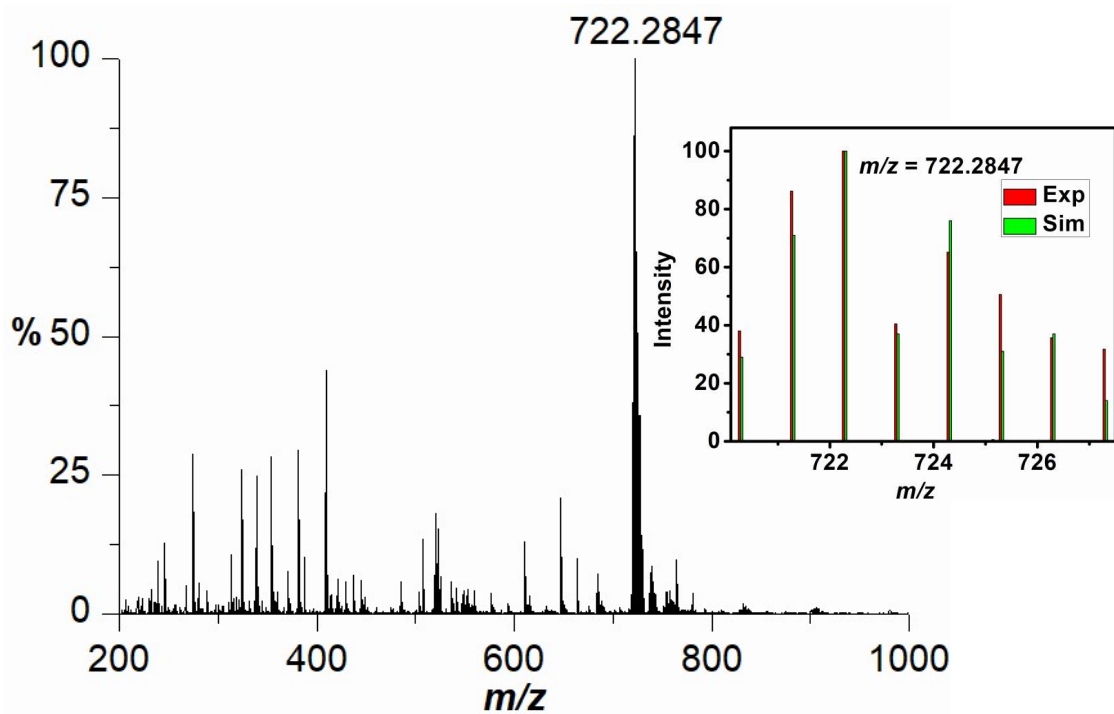
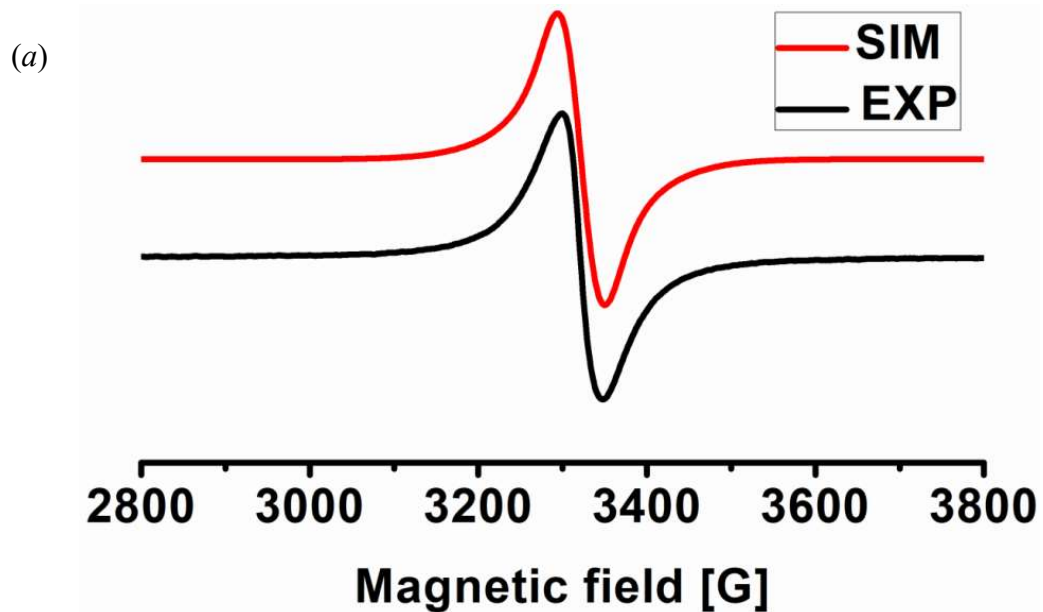


Fig. S11 Positive-Ion ESI-MS spectrum of $[\text{Pd}(\text{L}^*)]$ (4): $\{[\text{Pd}(\text{L}^*)] + \text{H}^+\}$. The isotope distribution patterns of the molecular ion peaks shown in insets.



(b)

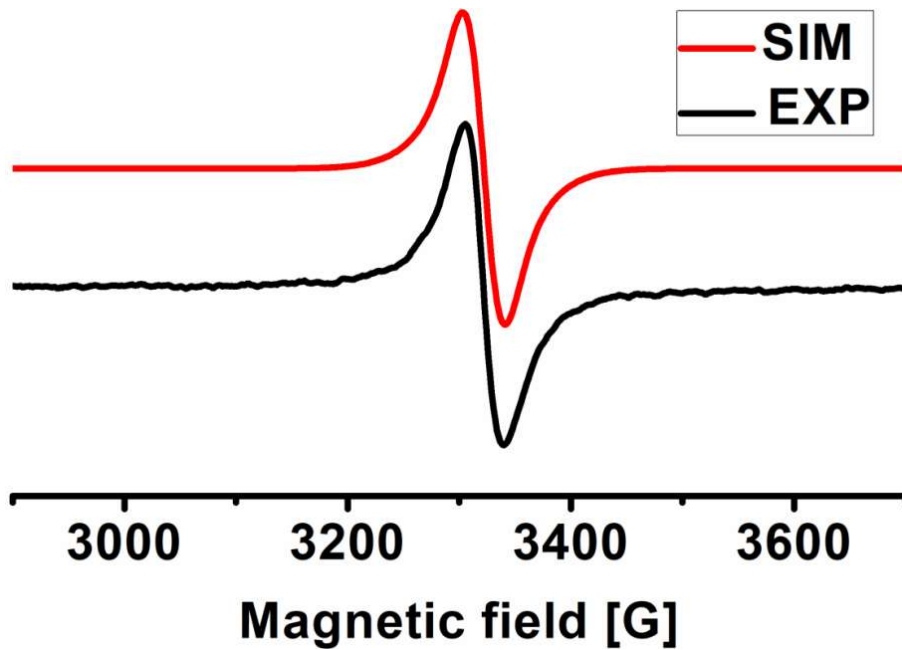


Fig. S12 X-band EPR spectrum ($\nu = 9.460$ GHz, power = 0.201 mW, receiver gain = 1×10^2 , modulation frequency = 100 KHz, modulation amplitude = 5.00 G) for 4 as solid recorded at (a) as solid at 298 K, upper trace: simulated parameters: $g_x = g_y = g_z = 2.00238$; $W_x = 40$ G, $W_y = 190$ G, $W_z = 45$ G; (b) as solid at 80 K, upper trace: simulated parameters: $g_x = g_y = g_z = 2.00232$; $W_x = 35$ G, $W_y = 105$ G, $W_z = 25$ G. Error limits: $g \pm 0.002$; $A \pm 0.0001$ cm $^{-1}$; $W \pm 1$.

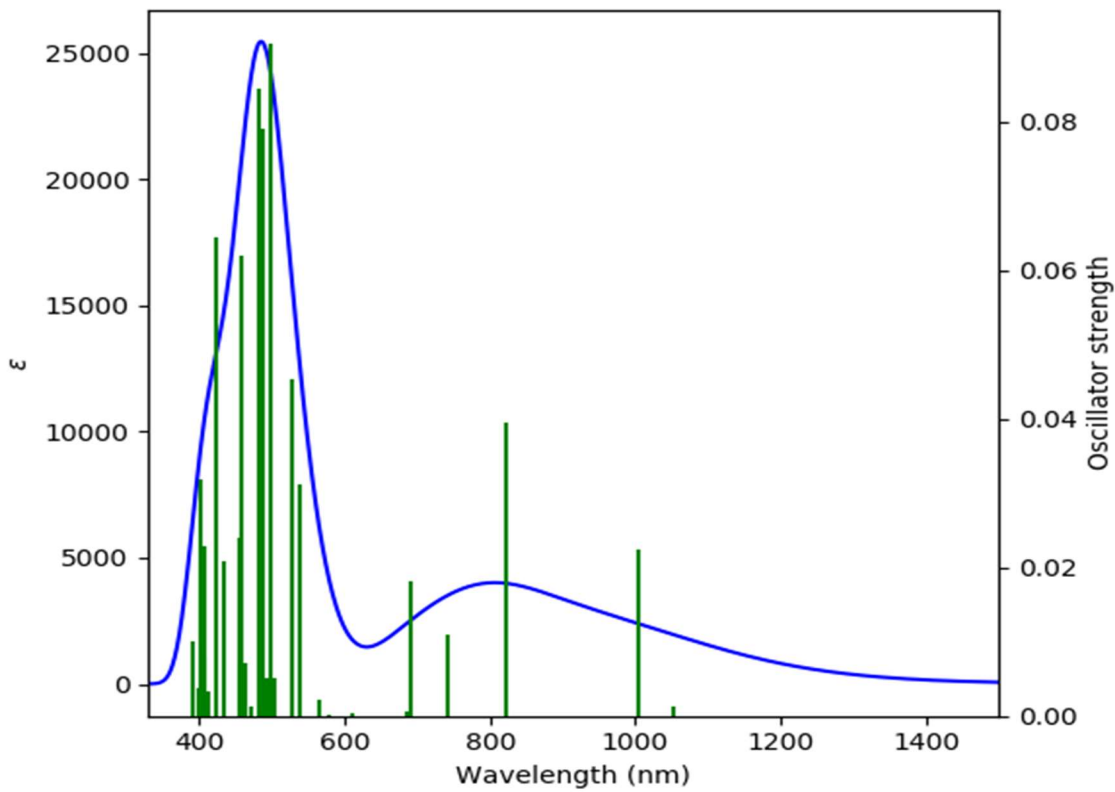
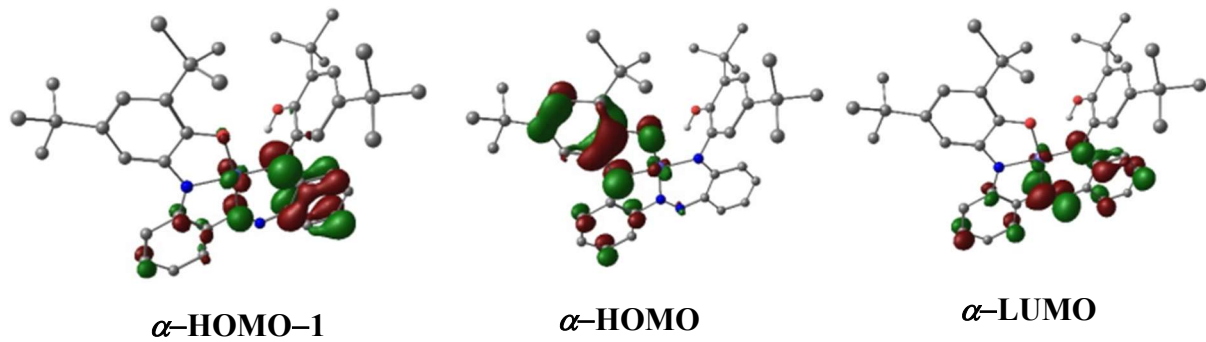


Fig. S13 TD-DFT calculated electronic spectra for $[\text{Ni}^{\text{II}}\{(\text{L}^{\text{ISQ}})^{2-}\}]$ (**1**).



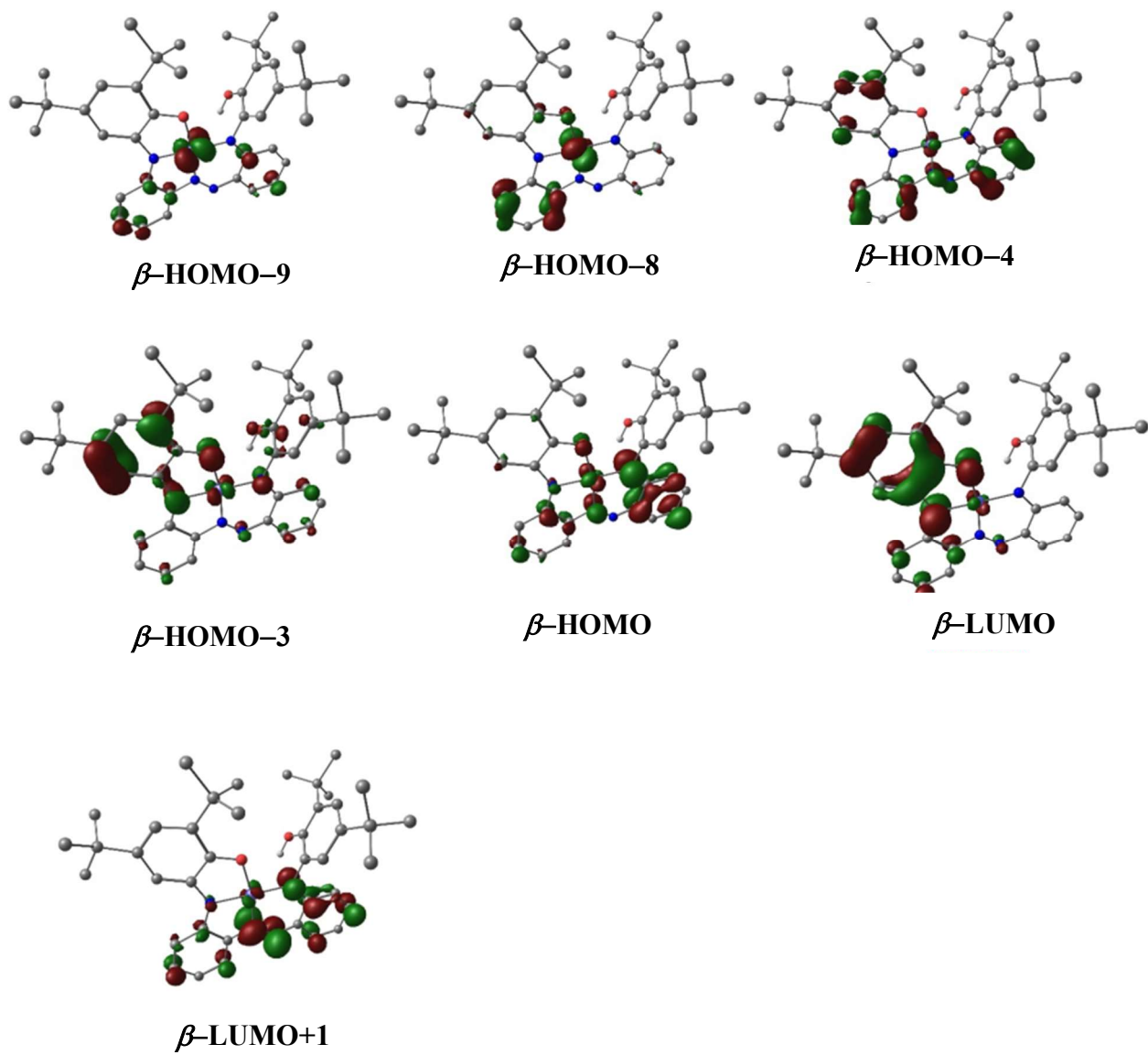


Fig. S14. Representative molecular orbitals involved in TD-DFT transitions of $[\text{Ni}^{\text{II}}\{(\text{L}^{\text{ISQ}})^{\cdot 2-}\}]$ (**1**).

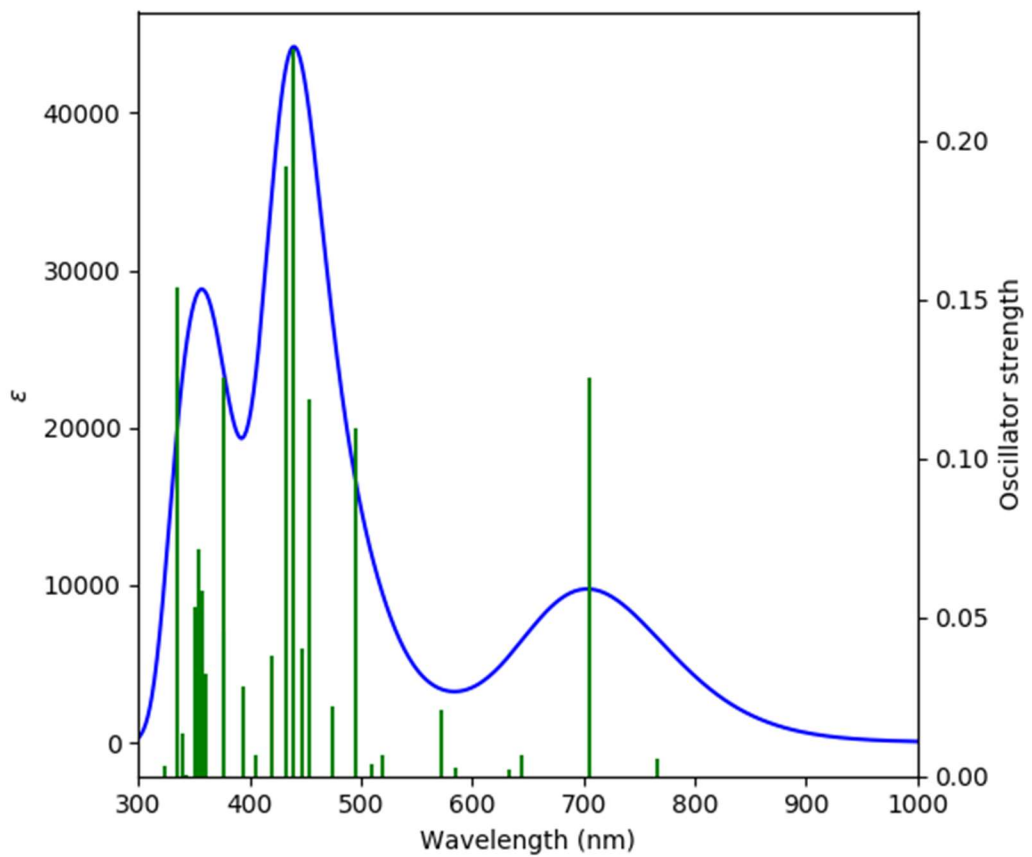
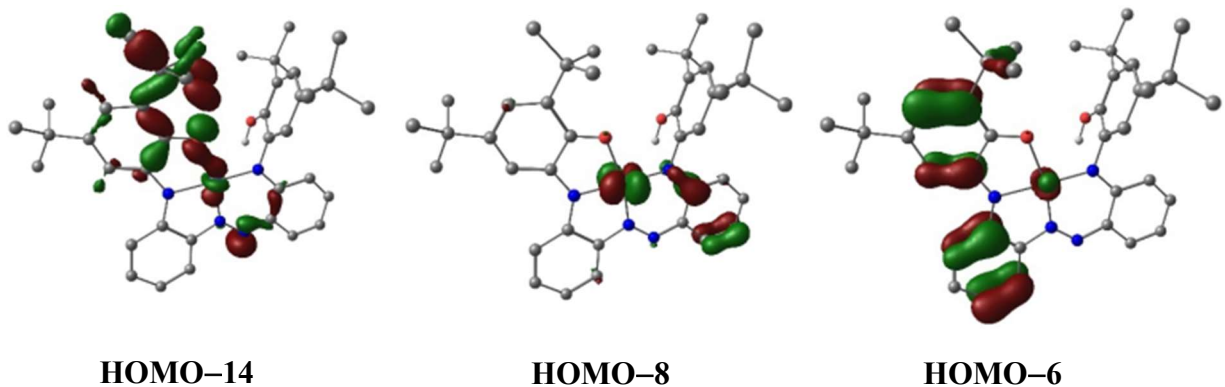


Fig. S15 TD-DFT calculated electronic spectra for $[\text{Ni}^{\text{II}}\{(\text{LIBQ})^{1-}\}]^{1+}$ (**1⁺/3**).



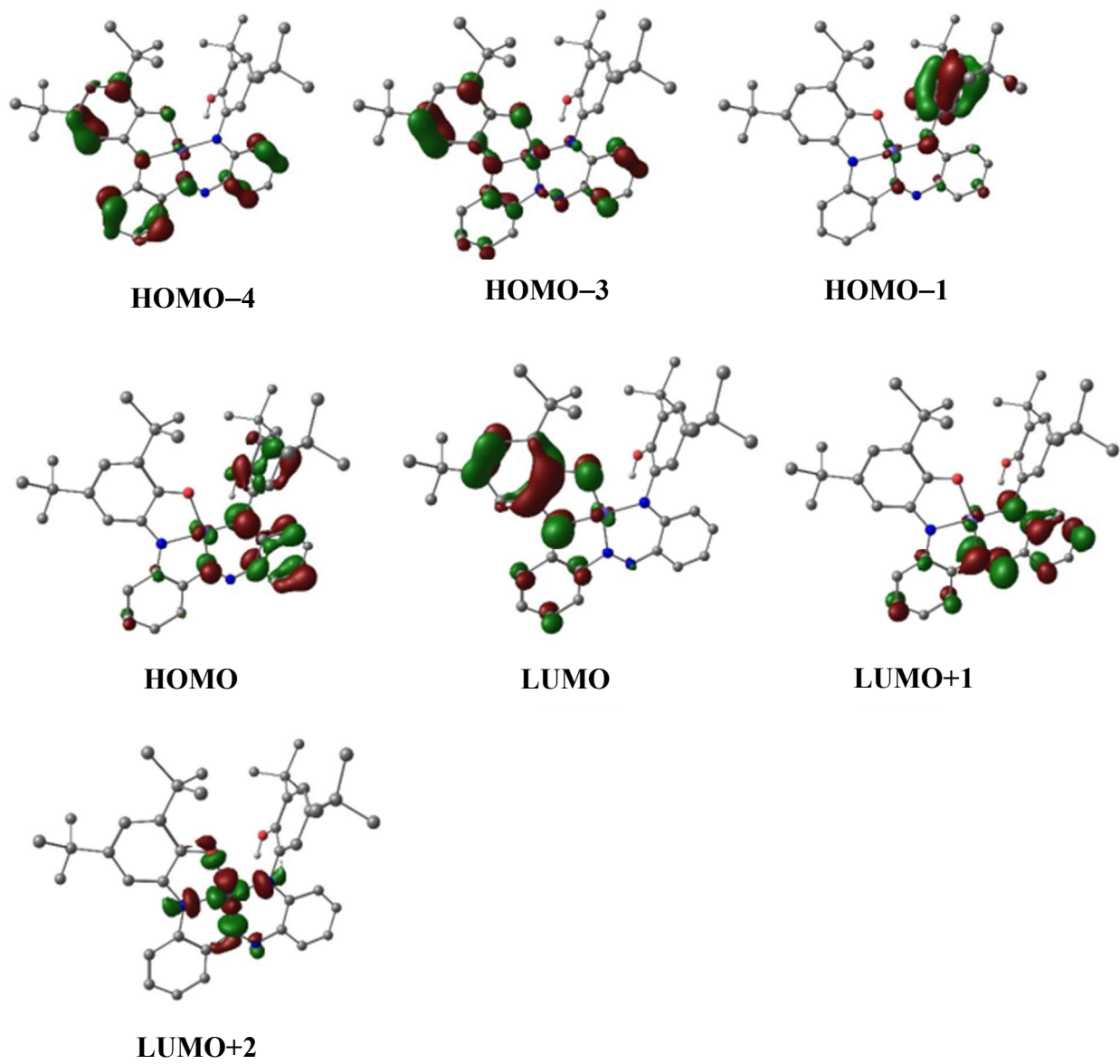


Fig. S16 Representative molecular orbitals involved in TD-DFT transitions of $[\text{Ni}^{\text{II}}\{(\text{L}^{\text{IBQ}})^{1-}\}]^{1+}$ ($1^+/3$).

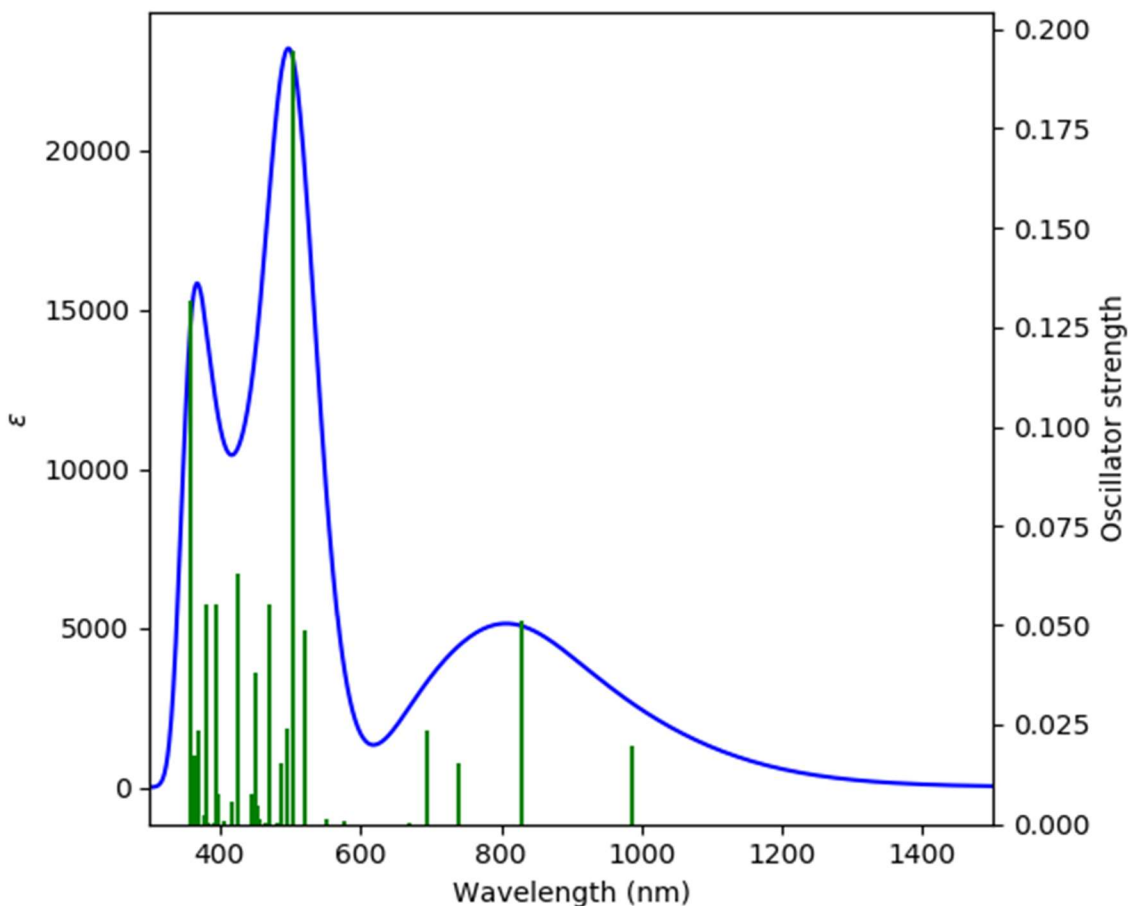
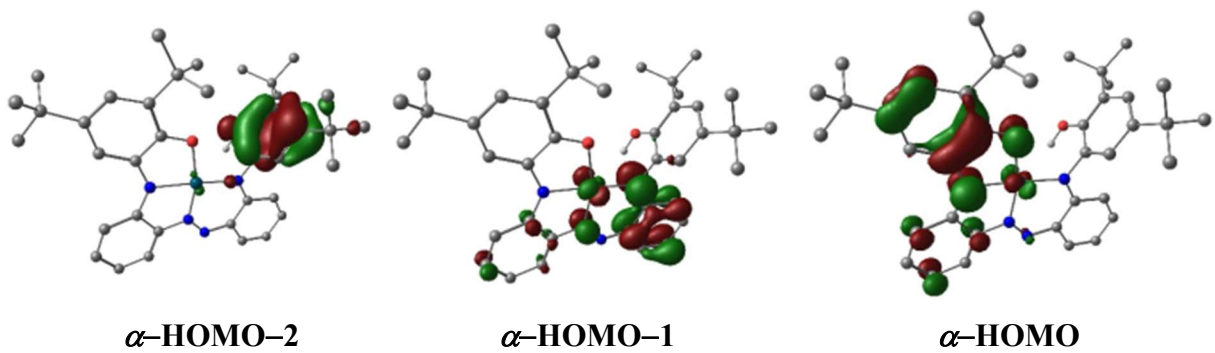


Fig. S17 TD-DFT calculated electronic spectra for $[\text{Pd}^{\text{II}}\{\text{L}^{\text{ISQ}}\}^{2-}\}]$ (**2**).



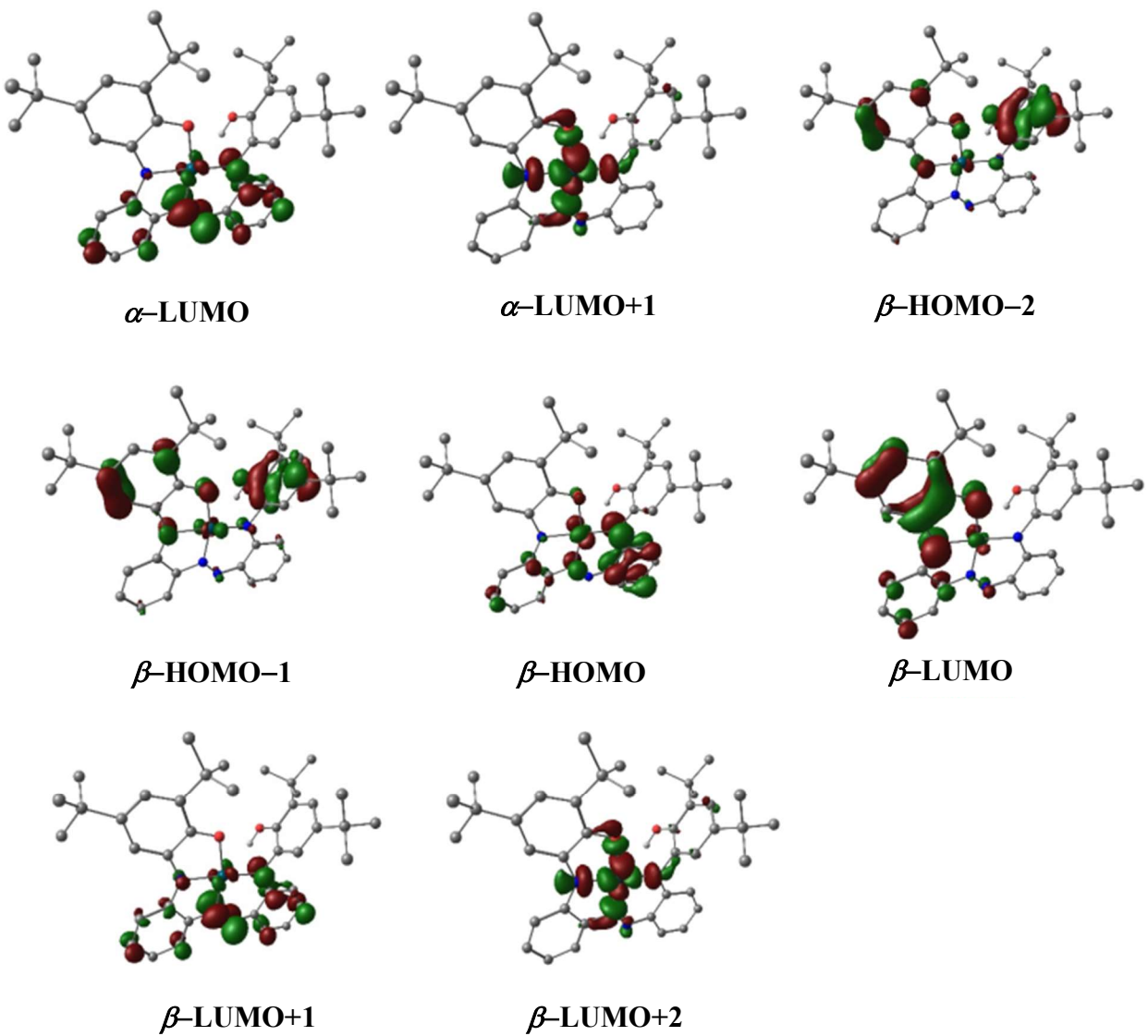


Fig. S18 Representative molecular orbitals involved in TD-DFT transitions of $[\text{Pd}^{\text{II}}\{(\text{L}^{\text{ISQ}})^{\cdot 2-}\}]$ (2).

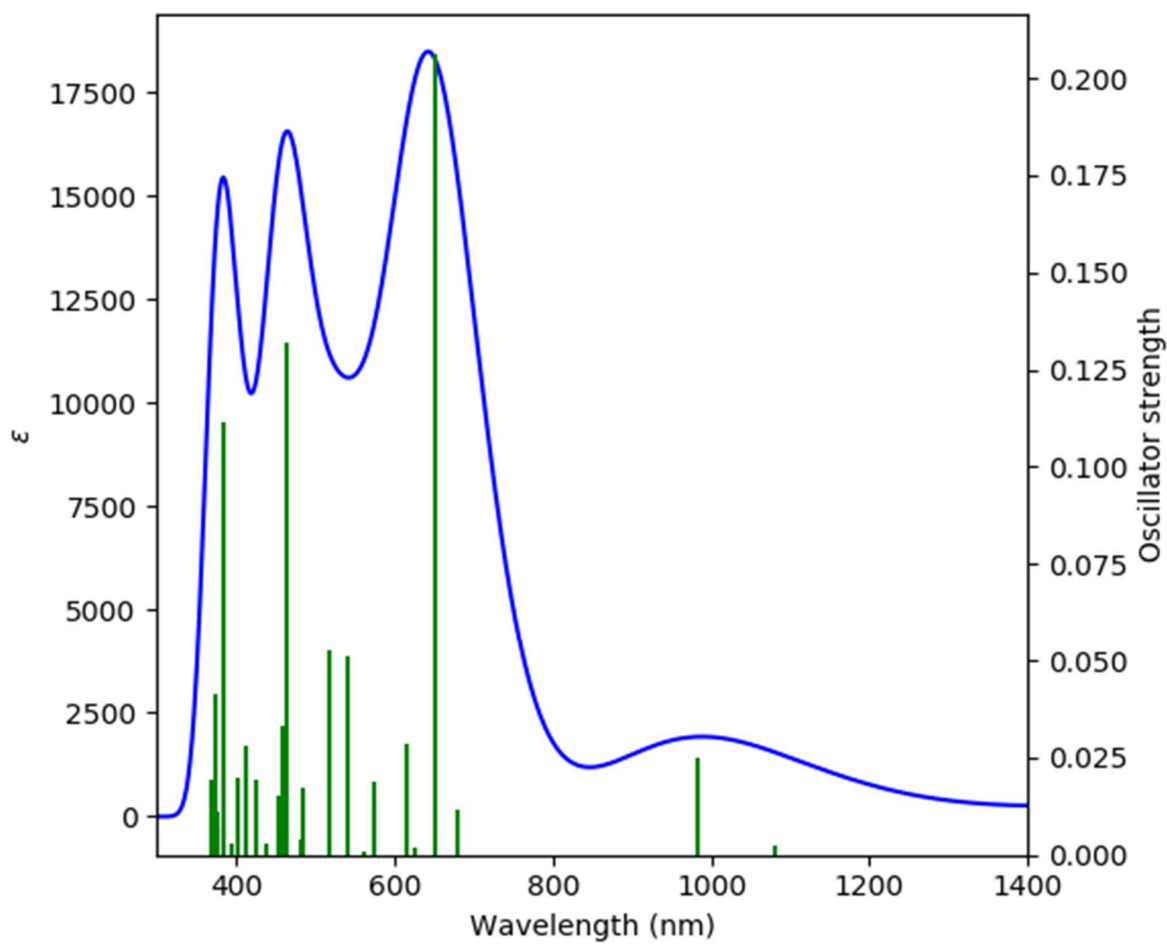
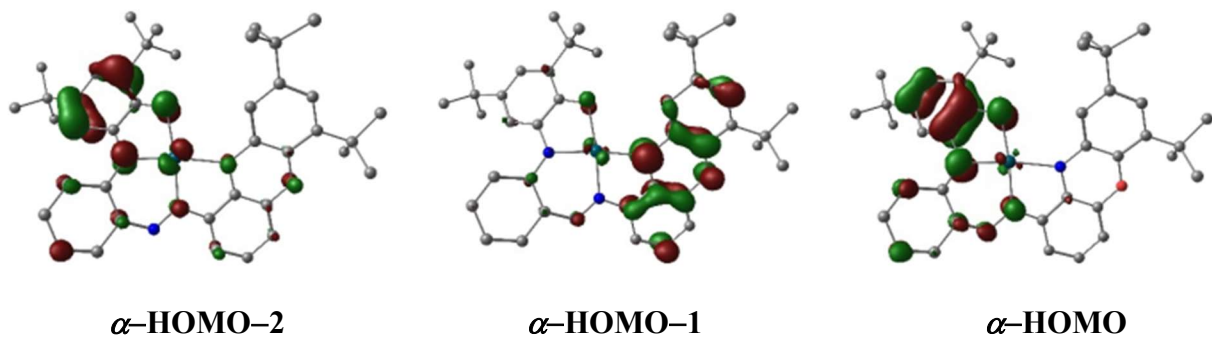


Fig. S19 TD-DFT calculated electronic spectra for $[\text{Pd}^{\text{II}}\{(\text{L}^{*\text{AP}})^{2-}\}]$ (4).



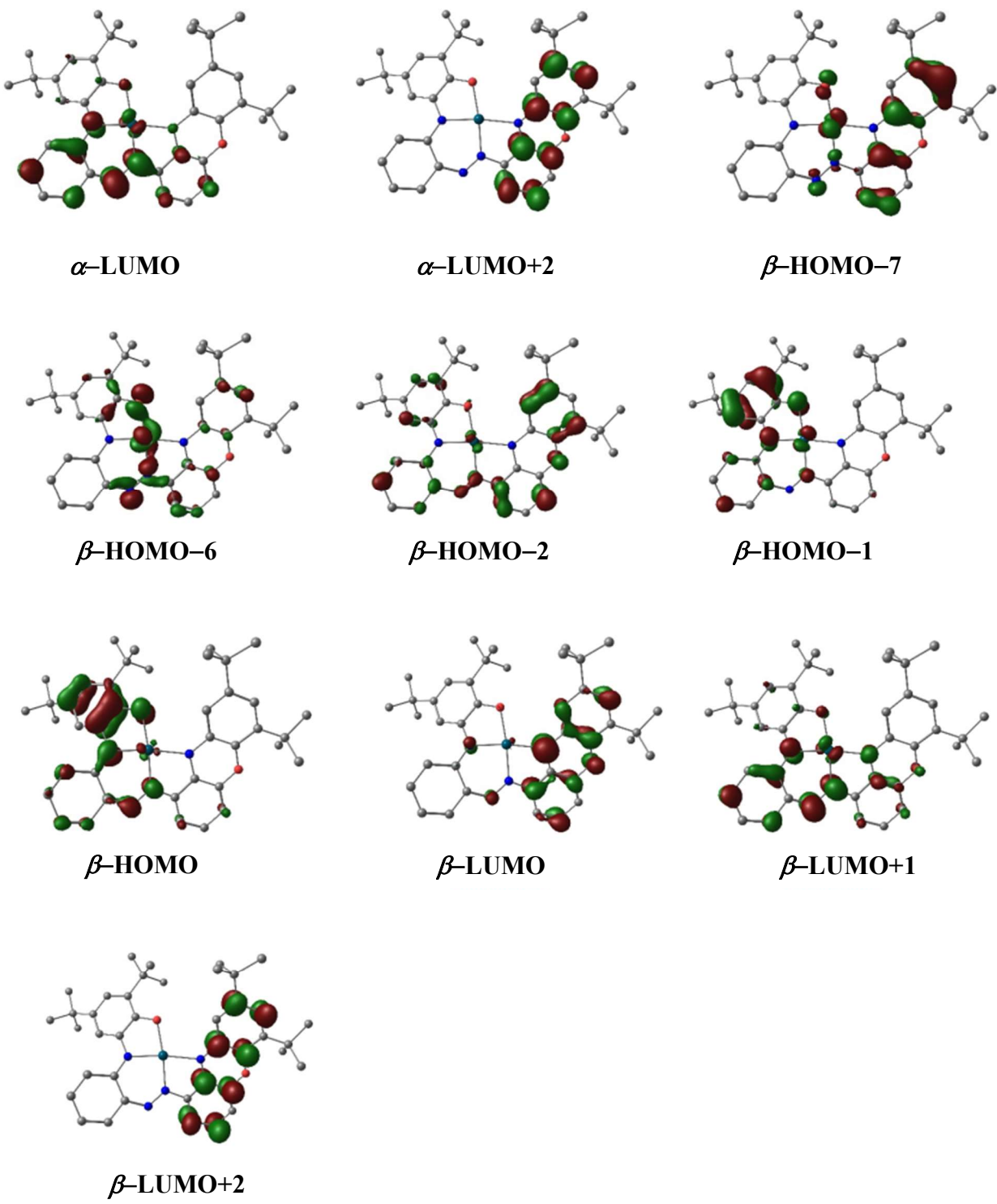


Fig. S20 Representative molecular orbitals involved in TD-DFT transitions of $[\text{Pd}^{\text{II}}\{\text{L}^{*\text{AP}}\}^{2-}]$ (4).

Table S1 Crystal data and structure refinement for **1–4**.

	1	2	3•2CH₂Cl₂	4
CCDC Number	2221416	2221418	2221417	2221419
Empirical formula	C ₄₀ H ₄₉ N ₄ O ₂ Ni	C ₄₀ H ₄₉ N ₄ NiO ₂ Pd	C ₈₄ H ₁₀₄ Cl ₈ F ₁₂ N ₈ Ni ₂ O ₄ Sb ₂	C ₈₀ H ₉₄ N ₈ O ₄ Pd ₂
Formula weight	676.52	724.23	2162.27	1444.43
Crystal color, habit	Violet	Pink	Red	Blue
Temperature (K)	100 (2)	100 (2)	100 (2)	100 (2)
Wavelength (Å)	MoKα ($\lambda = 0.71073$)	MoKα ($\lambda = 0.71073$)	MoKα ($\lambda = 0.71073$)	MoKα ($\lambda = 0.71073$)
Crystal system	triclinic	Triclinic	Triclinic	triclinic
Space group	<i>P</i> -1 (no. 2)	<i>P</i> -1 (no. 2)	<i>P</i> -1 (no. 2)	<i>P</i> -1 (no. 2)
<i>a</i> (Å)	9.6539(7)	9.6069(9)	9.5233(14)	13.9262(9)
<i>b</i> (Å)	11.1929(8)	11.3196(10)	18.212(3)	18.0565(11)
<i>c</i> (Å)	17.3192(12)	17.4614(16)	27.463(4)	18.0843(18)
α (°)	71.713(2)	72.042(3)	81.734(4)	103.105(2)
β (°)	81.597(2)	81.586(3)	83.363(4)	112.102(2)
γ (°)	89.058(2)	89.255(3)	85.055(4)	110.877(2)
Volume (Å ³)	1757.0(2)	1785.9(3)	4670.2(12)	3578.4(5)
Z	2	2	2	2
Density _{calc} (g cm ⁻³)	1.279	1.347	1.538	1.341
μ (mm ⁻¹)	0.589	0.559	1.274	0.558
no. reflcns colld	33677	28229	56507	56737
no. unique reflcns	8691	8862	16486	17980
no. reflcns used [$I > 2\sigma(I)$]	7104 [$R_{\text{int}} = 0.0556$, $R_{\text{sigma}} = 0.0551$]	7719 [$R_{\text{int}} = 0.0438$, $R_{\text{sigma}} = 0.0467$]	13430 [$R_{\text{int}} = 0.0546$, $R_{\text{sigma}} = 0.0547$]	14129 [$R_{\text{int}} = 0.0496$, $R_{\text{sigma}} = 0.0576$]
Goodness-of-fit on F^2	1.114	1.074	1.032	1.063
Final <i>R</i> indices [$I > 2\sigma(I)$] ^{a,b}	$R_1 = 0.0582^a$, $wR_2 = 0.1304^b$	$R_1 = 0.0376^a$, $wR_2 = 0.0824^b$	$R_1 = 0.0385^a$, $wR_2 = 0.0903^b$	$R_1 = 0.0421^a$, $wR_2 = 0.0828^b$
<i>R</i> indices (all data) ^{a,b}	$R_1 = 0.0764^a$, $wR_2 = 0.1392^b$	$R_1 = 0.0472^a$, $wR_2 = 0.0887^b$	$R_1 = 0.0513^a$, $wR_2 = 0.0983^b$	$R_1 = 0.0632^a$, $wR_2 = 0.0929^b$

^a $R_1 = \sum ||F_o| - |F_c|| / \sum |F_o|$. ^b $wR_2 = \{\sum [w(|F_o|^2 - |F_c|^2)^2] / \sum [w(|F_o|^2)^2]\}^{1/2}$.

Table S2 Selected bond angles (deg) for [Ni(L)] (**1**), [Pd(L)] (**2**), [Ni(L)]SbF₆•2CH₂Cl₂ (**3**•2CH₂Cl₂) and [Pd(L^{*})] (**4**).

1	3	2		4	
N1–Ni1–O1	85.20(10)	83.01(12)	N2–Pd–O1	168.07(7)	
N4–Ni1–O1	94.11(9)	96.16(13)	N2–Pd–N1	85.42(8)	
N4–Ni1–N1	179.23(12)	179.10(14)	N2–Pd–N4	92.84(8)	
N2–Ni1–O1	171.54(10)	169.31(13)	N1–Pd–O1	82.65(7)	
N2–Ni1–N1	86.36(10)	86.75(14)	N1–Pd–N4	178.25(8)	
N2–Ni1–N4	94.34(10)	94.11(14)	N4–Pd–O1	99.08(7)	
				O1–Pd1–N4	103.92(8)
				O1–Pd1–N3	173.62(8)
				N3–Pd1–N4	81.91(9)
				N3–Pd1–N1	91.14(9)
				O1–Pd1–N1	82.93(8)
				N1–Pd1–N4	172.75(9)

Table S3 X-ray Structural and DFT-Optimized Bond Lengths of **1–4**.

1	3
Ni–O1	1.868(2) [1.9219]
Ni–N1	1.856(2) [1.8831]
Ni–N2	1.823(2) [1.8612]
Ni–N4	1.846(2) [1.8902]
C1–O1	1.303(3) [1.2963]
C14–N1	1.362(4) [1.3555]
C15–N1	1.379(4) [1.3802]
C1–C14	1.444(4) [1.4545]
C14–C13	1.418(4) [1.4175]
C13–C8	1.362(4) [1.3808]
C8–C7	1.425(4) [1.4301]
C7–C2	1.376(4) [1.3824]
C2–C1	1.428(4) [1.4390]
N2–N3	1.290(3) [1.2740]
C20–N2	1.424(3) [1.4196]
C21–N3	1.364(4) [1.3515]
C26–N4	1.356(4) [1.3546]
C27–N4	1.443(3) [1.4358]
C40–O2	1.372(3) [1.3688]
	1.888(2) [1.9740]
	1.864(3) [1.9165]
	1.810(3) [1.8475]
	1.836(3) [1.8680]
	1.264(4) [1.2540]
	1.326(4) [1.3184]
	1.410(5) [1.3898]
	1.482(5) [1.5019]
	1.417(5) [1.4300]
	1.365(5) [1.3661]
	1.447(6) [1.4620]
	1.354(5) [1.3661]
	1.454(5) [1.4539]
	1.284(4) [1.2780]
	1.431(4) [1.4180]
	1.353(5) [1.3384]
	1.359(5) [1.3517]
	1.442(4) [1.4370]
	1.316(7) [1.3680]

2	4
Pd–O1	2.0167(16) [2.1063]
Pd–N1	1.9635(19) [2.0059]
Pd–N2	1.9256(19) [1.9682]
Pd–N4	1.9694(19) [2.0292]
Pd–N3	NA
C1–O1	1.301(3) [1.2936]
C14–N1	1.367(3) [1.3604]
C15–N1	1.386(3) [1.3844]
C1–C14	1.454(3) [1.4642]
C14–C13	1.418(3) [1.4183]
C13–C8	1.368(3) [1.3807]
	2.0336(18) [2.0658]
	1.954(2) [1.9952]
	NA
	2.085(2) [2.1361]
	1.949(2) [1.9903]
	1.331(3) [1.3246]
	1.406(3) [1.4017]
	1.351(3) [1.3437]
	1.422(4) [1.4311]
	1.397(4) [1.4062]
	1.387(4) [1.3897]

C8–C7	1.425(3) [1.4294]	1.410(4) [1.4096]
C7–C2	1.370(3) [1.3804]	1.393(4) [1.3956]
C2–C1	1.439(3) [1.4434]	1.422(4) [1.4287]
N2–N3	1.283(3) [1.2683]	1.293(3) [1.2890]
C20–N2	1.428(3) [1.4251]	1.353(3) [1.3452]
C21–N3	1.367(3) [1.3584]	1.401(3) [1.3923]
C26–N4	1.350(3) [1.3501]	1.372(3) [1.3611]
C27–N4	1.431(3) [1.4300]	1.387(3) [1.3797]
C40–O2	1.366(3) [1.3680]	1.377(3) [1.3753]
C25–O2	NA	1.361(3) [1.3627]
C21–C26	1.447(3)[1.4604]	1.412(4)[1.4256]
C21–C22	1.429(3)[1.4301]	1.389(4)[1.4005]
C22–C23	1.355(3)[1.3694]	1.38794)[1.3934]
C23–C24	1.409(4)[1.4159]	1.390(4)[1.4019]
C24–C25	1.364(3)[1.3741]	1.379(4)[1.3864]
C25–C26	1.431(3)[1.4342]	1.403(4)[1.4150]
C40–C27	1.392(3)[1.4045]	1.412(4)[1.4240]
C40–C35	1.401(3)[1.4127]	1.399(4)[1.4028]
C35–C34	1.397(3)[1.3995]	1.387(4)[1.4003]
C34–C29	1.399(3)[1.4068]	1.047(4)[1.4087]
C29–C28	1.393(3)[1.3946]	1.390(4)[1.3932]
C28–C27	1.394(3)[1.3981]	1.398(4)[1.4082]

Table S4 DFT-optimized cartesian coordinates of $[\text{Ni}^{\text{II}}\{(\text{L}^{\text{ISQ}})^{\cdot 2-}\}]$ (**1**)

Ni	6.733623000	5.732265000	6.489009000
O	6.886470000	6.465192000	4.718884000
N	5.510998000	7.142230000	6.740587000
O	6.709039000	2.711659000	4.293348000
H	6.417977000	3.071359000	5.144088000
N	7.898399000	4.265332000	6.235176000
N	6.395430000	5.310798000	8.270849000
N	6.835727000	4.369822000	9.008321000
C	5.055465000	7.271952000	8.036981000
C	5.519451000	6.238024000	8.894084000
C	5.189534000	7.819694000	5.611291000
C	8.244401000	3.377442000	7.197945000
C	11.813859000	5.059261000	3.161962000
C	7.702963000	3.443830000	8.542379000
C	4.007980000	9.387684000	4.190214000
C	7.916873000	3.285112000	3.999912000
C	9.764128000	4.707709000	4.688026000
H	10.190938000	5.335580000	5.461262000
C	8.532620000	4.106795000	4.956782000
C	4.269572000	8.299353000	8.600496000
H	3.970031000	9.150527000	8.006558000
C	8.085132000	2.478016000	9.522407000

H	7.643027000	2.591050000	10.506899000
C	2.888749000	10.400288000	3.898072000
C	8.961285000	1.464835000	9.236042000
H	9.241989000	0.738078000	9.990673000
C	10.422646000	4.477036000	3.479181000
C	6.931841000	7.858737000	2.104021000
C	4.146709000	8.758844000	5.411665000
H	3.438974000	8.944201000	6.203547000
C	6.053051000	7.434930000	4.505828000
C	5.955726000	8.142739000	3.256705000
C	4.945361000	9.080775000	3.154677000
H	4.839241000	9.615649000	2.219856000
C	7.929473000	2.047333000	1.733014000
C	9.790547000	3.626180000	2.554822000
H	10.301101000	3.426291000	1.621653000
C	12.285849000	6.053170000	4.240536000
H	11.593764000	6.895271000	4.345764000
H	13.264989000	6.459401000	3.966033000
H	12.393325000	5.574844000	5.219575000
C	12.839255000	3.901836000	3.087076000
H	12.891292000	3.363682000	4.039467000
H	13.840085000	4.287078000	2.859146000
H	12.573450000	3.179078000	2.309566000
C	6.666815000	8.763833000	0.884794000
H	5.670373000	8.603037000	0.458959000
H	7.396328000	8.533047000	0.102160000
H	6.771445000	9.826998000	1.127675000
C	9.156061000	2.298119000	6.951958000
H	9.581245000	2.201119000	5.961959000
C	9.493524000	1.387478000	7.926082000
H	10.186544000	0.588584000	7.675810000
C	5.151825000	6.188851000	10.239860000
H	5.518250000	5.378237000	10.857081000
C	6.794030000	6.388369000	1.644568000
H	7.029209000	5.696457000	2.452933000
H	7.482115000	6.192658000	0.814195000
H	5.775908000	6.185151000	1.294120000
C	8.550243000	3.012315000	2.766765000
C	6.537342000	2.551724000	1.281250000
H	5.847971000	2.639849000	2.121684000
H	6.107171000	1.850991000	0.556095000
H	6.617218000	3.529835000	0.796107000
C	11.790937000	5.802220000	1.805927000
H	11.510944000	5.141915000	0.979880000
H	12.783030000	6.209595000	1.579760000
H	11.079057000	6.632840000	1.827249000

C	8.804737000	1.912933000	0.470346000
H	8.933036000	2.870362000	-0.045856000
H	8.321010000	1.224529000	-0.230211000
H	9.796719000	1.507268000	0.695373000
C	4.340347000	7.192741000	10.762304000
H	4.053195000	7.163887000	11.808699000
C	8.379942000	8.123872000	2.583573000
H	8.497499000	9.162721000	2.912025000
H	9.079170000	7.952215000	1.757516000
H	8.651528000	7.461594000	3.407089000
C	3.918309000	8.249756000	9.946013000
H	3.315230000	9.049778000	10.364894000
C	7.794899000	0.636463000	2.359111000
H	8.776373000	0.249498000	2.655025000
H	7.367061000	-0.058236000	1.626927000
H	7.148918000	0.645553000	3.238325000
C	3.514909000	11.764804000	3.518647000
H	4.122676000	12.158350000	4.340009000
H	2.727507000	12.494266000	3.298236000
H	4.154833000	11.692357000	2.634548000
C	1.964546000	10.618799000	5.110552000
H	1.463090000	9.693661000	5.413407000
H	1.186946000	11.345474000	4.854907000
H	2.511289000	11.013518000	5.973521000
C	2.024001000	9.886727000	2.720617000
H	2.612859000	9.747850000	1.809365000
H	1.227102000	10.604308000	2.495425000
H	1.558022000	8.927191000	2.967286000

Table S5 DFT-optimized cartesian coordinates of $[\text{Ni}^{\text{II}}\{(\text{L}^{\text{IBQ}})^-\}]^{1+}$ (**1⁺/3**).

Ni	10.098746000	11.021574000	2.370786000
O	10.277371000	12.913001000	2.926307000
N	8.769283000	11.214796000	1.072851000
N	11.380170000	10.786313000	3.776411000
N	10.233512000	9.194749000	2.129857000
N	9.619795000	8.404073000	1.335202000
C	12.234586000	11.897150000	5.825225000
H	12.521403000	10.985569000	6.324660000
C	11.585620000	11.832121000	4.552532000
C	12.412942000	13.111709000	6.424715000
C	10.987295000	13.070017000	3.948037000
C	8.278845000	10.219341000	0.301098000
C	7.202320000	8.085667000	-1.311333000
H	6.781813000	7.301858000	-1.930944000
C	8.144020000	7.804952000	-0.362769000
H	8.506865000	6.797096000	-0.192639000

C	8.318183000	12.551917000	0.801316000
C	11.855538000	9.483753000	3.871632000
C	13.047610000	13.277486000	7.806265000
C	8.704676000	8.836925000	0.459700000
C	6.780094000	9.432034000	-1.471391000
H	6.027339000	9.667555000	-2.218232000
C	8.937963000	13.325010000	-0.181506000
C	7.292069000	10.454678000	-0.707270000
H	6.940869000	11.466549000	-0.858701000
C	11.194059000	8.595267000	2.983605000
C	7.199269000	13.037809000	1.502749000
C	12.916336000	9.003678000	4.666669000
H	13.505092000	9.679383000	5.270594000
C	11.287166000	14.366366000	4.547512000
C	11.976218000	14.319614000	5.726230000
H	12.205399000	15.257524000	6.213682000
C	13.432319000	11.927268000	8.437639000
H	12.562093000	11.277977000	8.579592000
H	13.873904000	12.099206000	9.422823000
H	14.176486000	11.391856000	7.838300000
C	8.451123000	14.595475000	-0.502726000
C	6.665395000	14.308866000	1.203460000
C	13.249078000	7.656362000	4.625656000
H	14.070326000	7.288112000	5.230893000
O	6.603566000	12.250965000	2.450203000
H	7.095295000	11.421356000	2.512437000
C	7.326762000	15.046438000	0.208605000
H	6.929991000	16.020428000	-0.035702000
C	12.538223000	6.776136000	3.796316000
H	12.802108000	5.723504000	3.777643000
C	10.833315000	15.675544000	3.888241000
C	11.517227000	7.238017000	2.968020000
H	10.987831000	6.572019000	2.299236000
C	11.410659000	15.756467000	2.453025000
H	12.505043000	15.710544000	2.463442000
H	11.122475000	16.711658000	2.003363000
H	11.028555000	14.957919000	1.815416000
C	12.036921000	13.988030000	8.744364000
H	11.758746000	14.983460000	8.386520000
H	12.484911000	14.110569000	9.735131000
H	11.121250000	13.399398000	8.857495000
C	14.329696000	14.140886000	7.672956000
H	15.063261000	13.661924000	7.016963000
H	14.786911000	14.264268000	8.659430000
H	14.125697000	15.141422000	7.281376000
C	9.287029000	15.725673000	3.839237000

H	8.870569000	14.919027000	3.235640000
H	8.971207000	16.674595000	3.394226000
H	8.860123000	15.669174000	4.846087000
C	5.380909000	14.832166000	1.885310000
C	11.331186000	16.902956000	4.675683000
H	10.916398000	16.943351000	5.688665000
H	11.007337000	17.810894000	4.160042000
H	12.424038000	16.938562000	4.742353000
C	5.560103000	14.906084000	3.421455000
H	5.802517000	13.934245000	3.853345000
H	4.631398000	15.259741000	3.882144000
H	6.352075000	15.614106000	3.687064000
C	4.200386000	13.888794000	1.541164000
H	4.038757000	13.849068000	0.458502000
H	3.280163000	14.262924000	2.002682000
H	4.372391000	12.873795000	1.902890000
C	5.004616000	16.245949000	1.396875000
H	5.787373000	16.980483000	1.614374000
H	4.097501000	16.572380000	1.914013000
H	4.793573000	16.272076000	0.322993000
C	9.086788000	15.403143000	-1.652685000
C	8.531931000	16.838530000	-1.735960000
H	9.040965000	17.382451000	-2.537434000
H	7.461490000	16.855623000	-1.963755000
H	8.693276000	17.392660000	-0.805085000
C	8.780610000	14.683808000	-2.989593000
H	9.215002000	15.235931000	-3.830127000
H	9.195020000	13.670611000	-3.005567000
H	7.701084000	14.608460000	-3.156015000
C	10.619198000	15.495695000	-1.469956000
H	10.876128000	16.011408000	-0.539404000
H	11.096246000	14.510875000	-1.453094000
H	11.063161000	16.056835000	-2.298945000
H	9.784076000	12.894507000	-0.707853000

Table S6 DFT-optimized cartesian coordinates of $[\text{Pd}^{\text{II}}\{(\text{L}^{\text{ISQ}})^{\cdot 2-}\}]$ (**2**).

Pd	6.761324000	5.713512000	6.479379000
O	6.831624000	6.604527000	4.572128000
N	6.380237000	5.317362000	8.369327000
N	7.970860000	4.093224000	6.307602000
N	6.804885000	4.377246000	9.107223000
N	5.495221000	7.243470000	6.762070000
O	6.787447000	2.538648000	4.369358000
H	6.500640000	2.885669000	5.227072000
C	5.514861000	6.293098000	8.943748000
C	5.137734000	6.261781000	10.288886000

H	5.479744000	5.440598000	10.906264000
C	3.894828000	9.509365000	4.286691000
C	7.663898000	3.419932000	8.670079000
C	8.250110000	3.270305000	7.340849000
C	5.076671000	7.344557000	8.077884000
C	4.790451000	9.240615000	3.205559000
H	4.639291000	9.794081000	2.287912000
C	5.154036000	7.922954000	5.633952000
C	8.002633000	2.485109000	9.697996000
H	7.536847000	2.650343000	10.663875000
C	5.809080000	8.309897000	3.246773000
C	8.625302000	3.906281000	5.049965000
C	9.145599000	2.161696000	7.179041000
H	9.595007000	2.016291000	6.204919000
C	9.435397000	1.289915000	8.200997000
H	10.118290000	0.466487000	8.009348000
C	5.974663000	7.568686000	4.474204000
C	8.602390000	2.891725000	2.821899000
C	9.853689000	4.517494000	4.781185000
H	10.287165000	5.129627000	5.563198000
C	9.836258000	3.516984000	2.608923000
H	10.323819000	3.362573000	1.654800000
C	4.094266000	8.853771000	5.485410000
H	3.413979000	9.009473000	6.307043000
C	6.730825000	8.043498000	2.043082000
C	4.358297000	7.287357000	10.814404000
H	4.070694000	7.264502000	11.860700000
C	7.993708000	3.114054000	4.077234000
C	2.746301000	10.507779000	4.067658000
C	4.328743000	8.394407000	8.655354000
H	4.062137000	9.257183000	8.062533000
C	6.412041000	8.975301000	0.857078000
H	5.397254000	8.823853000	0.473269000
H	7.105204000	8.762368000	0.037265000
H	6.528461000	10.032750000	1.118764000
C	10.487178000	4.332443000	3.552623000
C	3.974796000	8.359065000	9.999418000
H	3.401361000	9.181181000	10.417038000
C	7.950143000	1.985200000	1.756002000
C	8.863784000	1.441329000	9.487525000
H	9.103784000	0.746613000	10.285095000
C	11.850407000	4.963178000	3.211007000
C	11.711798000	5.864782000	1.961475000
H	11.363505000	5.302591000	1.089782000
H	12.678940000	6.311838000	1.703450000
H	10.999068000	6.675679000	2.142325000

C	6.561709000	6.583365000	1.555438000
H	6.840068000	5.869909000	2.331328000
H	7.200041000	6.410260000	0.681243000
H	5.524895000	6.390811000	1.257785000
C	6.561827000	2.540179000	1.353783000
H	5.885840000	2.593094000	2.208008000
H	6.107669000	1.891336000	0.595731000
H	6.655178000	3.543707000	0.925759000
C	8.802676000	1.895266000	0.474223000
H	8.932648000	2.872028000	-0.003855000
H	8.299892000	1.241919000	-0.246163000
H	9.793680000	1.470462000	0.665905000
C	8.204310000	8.290222000	2.452006000
H	8.348311000	9.324200000	2.785231000
H	8.860065000	8.121408000	1.590146000
H	8.510222000	7.617647000	3.254597000
C	1.865669000	10.674281000	5.320086000
H	1.397419000	9.730313000	5.617942000
H	1.062259000	11.388491000	5.113348000
H	2.436152000	11.060277000	6.171595000
C	7.797769000	0.549035000	2.316389000
H	8.776000000	0.128770000	2.575371000
H	7.343194000	-0.100818000	1.559618000
H	7.167562000	0.527951000	3.206711000
C	12.395753000	5.825693000	4.364882000
H	11.720662000	6.652754000	4.608119000
H	13.359913000	6.258801000	4.078993000
H	12.556038000	5.236070000	5.273638000
C	12.878920000	3.844007000	2.920630000
H	13.007142000	3.195122000	3.793474000
H	13.855111000	4.276240000	2.671963000
H	12.570686000	3.214663000	2.080253000
C	3.332330000	11.894192000	3.703480000
H	3.966171000	12.275511000	4.510766000
H	2.523699000	12.614554000	3.536471000
H	3.936846000	11.858647000	2.792626000
C	1.845647000	10.010911000	2.910169000
H	2.400592000	9.908529000	1.973204000
H	1.028060000	10.719500000	2.736720000
H	1.406624000	9.036320000	3.147136000

Table S7 DFT-optimized cartesian coordinates of $[Pd^{II}\{(\text{L}^{\text{*AP}})^{\bullet 2-}\}]$ (4).

Pd	5.780779000	4.500217000	5.425370000
O	6.218855000	5.537226000	3.693189000
O	5.196251000	7.525675000	9.243709000
N	5.572724000	3.328445000	7.020671000

N	5.380793000	5.995026000	6.898053000
N	5.484517000	2.042839000	7.052227000
N	6.174746000	2.937324000	4.249258000
C	5.446938000	5.419745000	8.129907000
C	5.451726000	5.580734000	10.572463000
H	5.399825000	6.197930000	11.462136000
C	5.577286000	4.004189000	8.238031000
C	5.747365000	1.700715000	4.555638000
C	5.358093000	6.174914000	9.323268000
C	5.466600000	1.292045000	5.936191000
C	7.590943000	2.464132000	2.266188000
H	7.714341000	1.433788000	2.575195000
C	8.211019000	2.925425000	1.111097000
C	4.790035000	7.947674000	5.594445000
H	4.907553000	7.333582000	4.707939000
C	5.513118000	0.707123000	3.543797000
H	5.592054000	1.014908000	2.509298000
C	5.057762000	7.334915000	6.833760000
C	6.834551000	3.329567000	3.076394000
C	6.783119000	4.733608000	2.804049000
C	5.139955000	-0.081984000	6.192939000
H	4.986947000	-0.346998000	7.233692000
C	5.661834000	3.399406000	9.498419000
H	5.765799000	2.323866000	9.557420000
C	4.580173000	9.463294000	8.002992000
C	5.139920000	-0.576491000	3.843897000
H	4.941306000	-1.272962000	3.034032000
C	9.056340000	1.960706000	0.256238000
C	10.266371000	1.466829000	1.085317000
H	10.901584000	2.306593000	1.385913000
H	10.877358000	0.769574000	0.499720000
H	9.947727000	0.949410000	1.995447000
C	5.608470000	4.189437000	10.645043000
H	5.682821000	3.717164000	11.619533000
C	4.942634000	8.108262000	8.023946000
C	4.376635000	9.276794000	5.534125000
C	4.985157000	-0.999219000	5.192238000
H	4.715171000	-2.025501000	5.418289000
C	8.051524000	4.289389000	0.792819000
H	8.513375000	4.655853000	-0.112288000
C	4.296193000	9.999256000	6.740813000
H	3.991399000	11.033101000	6.694342000
C	4.041425000	9.938935000	4.183260000
C	5.848976000	10.359239000	10.008619000
H	6.183016000	9.368922000	10.320731000
H	5.777328000	10.989676000	10.901802000

H	6.615746000	10.789416000	9.355623000
C	7.367822000	5.208567000	1.590023000
C	9.592957000	2.626516000	-1.025795000
H	8.781667000	2.989316000	-1.665822000
H	10.170983000	1.898535000	-1.604773000
H	10.255792000	3.469087000	-0.803761000
C	8.199329000	0.743065000	-0.165035000
H	7.828576000	0.186306000	0.701120000
H	8.790723000	0.049439000	-0.774006000
H	7.332981000	1.059764000	-0.755362000
C	3.396390000	9.733666000	10.232834000
H	2.420074000	9.712223000	9.737118000
H	3.305832000	10.363893000	11.124554000
H	3.636521000	8.721074000	10.559351000
C	4.478036000	10.314709000	9.288420000
C	5.799790000	7.107148000	1.079179000
H	5.3074448000	6.536249000	0.284036000
H	5.715031000	8.171312000	0.830595000
H	5.265175000	6.922171000	2.011937000
C	8.007317000	7.553374000	2.265923000
H	7.561629000	7.416584000	3.252485000
H	7.957878000	8.615386000	1.997401000
H	9.065063000	7.274093000	2.328038000
C	7.285753000	6.694578000	1.198865000
C	4.078553000	11.772200000	8.976093000
H	4.807502000	12.270287000	8.328537000
H	4.031867000	12.337091000	9.912098000
H	3.092805000	11.840288000	8.504374000
C	3.096817000	9.025178000	3.368497000
H	3.541489000	8.049896000	3.158626000
H	2.861842000	9.492101000	2.405932000
H	2.155386000	8.859567000	3.903212000
C	7.954150000	6.988493000	-0.159497000
H	9.027183000	6.769337000	-0.149854000
H	7.840852000	8.052432000	-0.392806000
H	7.494651000	6.422178000	-0.976695000
C	5.357082000	10.163087000	3.402996000
H	6.027195000	10.832147000	3.953725000
H	5.150282000	10.618286000	2.427599000
H	5.886065000	9.223880000	3.233240000
C	3.341412000	11.302740000	4.351570000
H	2.418821000	11.220226000	4.936208000
H	3.075172000	11.695859000	3.365391000
H	3.987622000	12.046544000	4.829116000

Table S8 TD-DFT-calculated electronic transitions of of $[\text{Ni}^{\text{II}}\{(\text{L}^{\text{ISQ}})^{\cdot 2-}\}] (\mathbf{1})$.

Excitation energy(eV)	λ (nm)	f	Transition	Character
1.1957	1003	0.0225	$\beta\text{-H}[\sim 89\%\text{L}] \rightarrow \beta\text{-L}[\sim 94\%\text{L}]$ (80%)	MLCT (Metal \rightarrow iminosemiquinonate ring) CT (azo appended amidophenyl ring \rightarrow iminosemiquinonate ring)
1.4586	822	0.0396	$\alpha\text{-H-1}[\sim 84\%\text{L}] \rightarrow \alpha\text{-L}[\sim 95\%\text{L}]$ (13%) $\beta\text{-H-2}[\sim 90\%\text{L}] \rightarrow \beta\text{-L}[\sim 94\%\text{L}]$ (57%)	CT (azo appended amidophenyl ring \rightarrow azo) MLCT (metal \rightarrow azo) CT (amido phenol \rightarrow iminosemiquinonate ring and amido phenyl ring)
1.6146	743	0.0109	$\alpha\text{-H-1}[\sim 84\%\text{L}] \rightarrow \alpha\text{-L}[\sim 95\%\text{L}]$ (37%) $\beta\text{-H-2}[\sim 90\%\text{L}] \rightarrow \beta\text{-L}[\sim 94\%\text{L}]$ (12%) $\beta\text{-H}[\sim 89\%\text{L}] \rightarrow \beta\text{-L+1}[\sim 95\%\text{L}]$ (30%)	CT (azophenyl ring \rightarrow azo) MLCT (metal \rightarrow azo) CT (amido phenol \rightarrow iminosemiquinonate ring and amido phenyl ring) CT (iminosemiquinonato O and N \rightarrow azo) MLCT (metal \rightarrow azo)
1.7351	691	0.0181	$\alpha\text{-H}[\sim 93\%\text{L}] \rightarrow \alpha\text{-L}[\sim 95\%\text{L}]$ (91%)	CT (iminosemiquinonate ring \rightarrow azo and azo appended amidophenyl ring)
2.4137	497	0.0906	$\alpha\text{-H-1}[\sim 84\%\text{L}] \rightarrow \alpha\text{-L}[\sim 95\%\text{L}]$ (17%) $\beta\text{-H-4}[\sim 94\%\text{L}] \rightarrow \beta\text{-L}[\sim 94\%\text{L}]$ (17%) $\beta\text{-H}[\sim 89\%\text{L}] \rightarrow \beta\text{-L+1}[\sim 95\%\text{L}]$ (30%)	CT (azoamidophenyl ring \rightarrow azo) MLCT (metal \rightarrow azo) CT (azo and azo appended amidophenyl ring \rightarrow iminosemiquinonate ring) CT (iminosemiquinonato O and N \rightarrow azo) MLCT (metal \rightarrow azo)
2.8339	423	0.0645	$\beta\text{-H-9}[\sim 72\%\text{M}] \rightarrow \beta\text{-L}[\sim 94\%\text{L}]$ (11%) $\beta\text{-H-8}[\sim 60\%\text{M}] \rightarrow \beta\text{-L}[\sim 94\%\text{L}]$ (73%)	MLCT (metal \rightarrow iminosemiquinonate ring) MLCT (metal \rightarrow iminosemiquinonate ring)

^aH and L stands for KS-HOMO and KS-LUMO, respectively.^bCT and MLCT stands for charge transfer and metal-to-ligand chanrge transfer, respectively.**Table S9** TD-DFT-calculated electronic transitions of $[\text{Ni}^{\text{II}}\{(\text{L}^{\text{IBQ}})^{\cdot -}\}]^{1+}$ (**1⁺/3**).

Excitation energy(eV)	λ (nm)	f	Transition	Character
1.7002	705	0.1252	$\text{H-3}[\sim 90\%\text{L}] \rightarrow \text{L+2}[\sim 40\%\text{M}]$ (87%)	LMCT (iminoquinone ring, azo and azo appended amido phenyl ring \rightarrow metal)

2.4191	496	0.1095	H-1[~96%L]→ L+1[~96%L](25%) H[~91%L]→ L+1[~96%L](43%)	CT (amido phenol ring → azo and azo appended amido phenyl ring) CT (amido phenol ring → azo)
2.6443	453	0.1188	H-1[~96%L]→ L+2[~40%M](59%) H[~91%L]→ L+2[~40%M](14%)	LMCT (amido phenol ring → metal) LMCT (amido phenol ring and azo appended amido phenyl ring → metal)
2.7359	438	0.2291	H-8[~66%M]→ L[~94%L](24%) H-6[~90%L]→ L[~94%L](50%)	MLCT (metal → iminoquinone ring) CT (amido phenyl ring → iminoquinone ring)
3.1842	376	0.1254	H-14[~86%L]→ L [~94%L] (20%) H-3[~90%L]→ L+1 [~96%L] (63%)	CT (tert-butyl moiety of iminoquinone ring → iminoquinone) and minor MLCT (metal → iminoquinone) CT (iminoquinone ring → azo and azo appended amido phenyl ring)
3.5768	335	0.1537	H-4[~97%L]→ L+1[~96%L] (88%)	CT (iminoquinone ring → azo and azo appended amido phenyl ring)

^aH and L stands for KS-HOMO and KS-LUMO, respectively.

^bCT , MLCT and LMCT stands for charge transfer, metal-to-ligand chanrge transfer and ligand-to-metal chanrge transfer, respectively.

Table S10 TD-DFT-calculated electronic transitions of $[\text{Pd}^{\text{II}}\{\text{(L}^{\text{ISQ}})^{\cdot 2-}\}]$ (2).

Excitation energy(eV)	λ (nm)	f	Transition	Character
1.2165	986	0.0196	β -H[~89%L]→ β -L[~95%L](81%)	CT (azo and azo appended amido phenyl ring→ iminosemiquononate ring) and minor MLCT (Metal → iminosemiquononate ring)
1.4486	828	0.0513	α -H-1[~88%L]→ α -L[~94%L](14%) β -H-2[~95%L]→ β -L[~95%L](27%) β -H[~89%L]→ β -L[~95%L](43%)	CT (azo appended amido phenyl ring → azo) and minor MLCT (metal → azo) CT (amido phenol ring → iminosemiquononate ring) CT (azo and azo appended amido phenyl ring →)

				iminosemiquinonate ring)
1.6214	740	0.0152	α -H-1[~88%L]→ α -L[~94%L](37%) β -H[~89%L]→ β -L[~95%L](15%) β -H[~89%L]→ β -L+1[~94%L](27%)	CT (azo appended amido phenyl ring → azo) and minor MLCT (metal → azo) CT (azo and azo appended amido phenyl ring → iminosemiquinonate ring) CT (azo appended amido phenyl ring → azo)
1.7302	693	0.0233	α -H[~93%L]→ α -L[~94%L](91%)	CT (iminosemiquinonate ring → azo and azo appended amido phenyl ring)
2.3812	503	0.1947	α -H-1[~88%L]→ α -L[~94%L](37%) β -H[~89%L]→ β -L+1[~94%L](44%)	CT (azo appended amido phenyl ring → azo) and minor MLCT (metal → azo) CT (azo appended amido phenyl ring → azo)
3.3513	358	0.1318	α -H-2[~97%L]→ α -L+1[~60%L](21%) β -H-2[~95%L]→ β -L+2[~62%L](23%)	LMCT (amido phenol ring → metal) LMCT (amido phenol ring → metal)

^aH and L stands for KS-HOMO and KS-LUMO, respectively.

^bCT , MLCT and LMCT stands for charge transfer, metal-to-ligand chanrge transfer and ligand-to-metal chanrge transfer, respectively.

Table S11 TD-DFT-calculated electronic transitions of $[\text{Pd}^{\text{II}}\{\text{(L}^{*\text{AP}}\text{)}^{\cdot 2-}\}]$ (4).

Excitation energy(eV)	λ (nm)	f	Transition	Character
1.2197	983	0.0247	α -H[~95%L]→ α -L[~94%L](25%) β -H-1[~90%L]→ β -L[~98%L](46%) β -H[~95%L]→ β -L+1[~94%L](24%)	CT (amidophenolate ring→ azo and amidophenyl ring) CT (amidophenolate ring → phenoxyazine-ring) CT (amidophenolate ring → phenoxyazine-ring)
1.7649	679	0.0116	β -H-2[~96%L]→ β -L[~98%L](84%)	CT (azo and amidophenolate moiety→ phenoxyazine-ring)
1.8408	651	0.2064	α -H[~95%L]→ α -L[~94%L](36%) β -H[~95%L]→ β -L+1[~94%L](45%)	CT (amido phenyl → amido phenolate ring) CT (amidophenolate ring→ azo and amidophenyl ring)

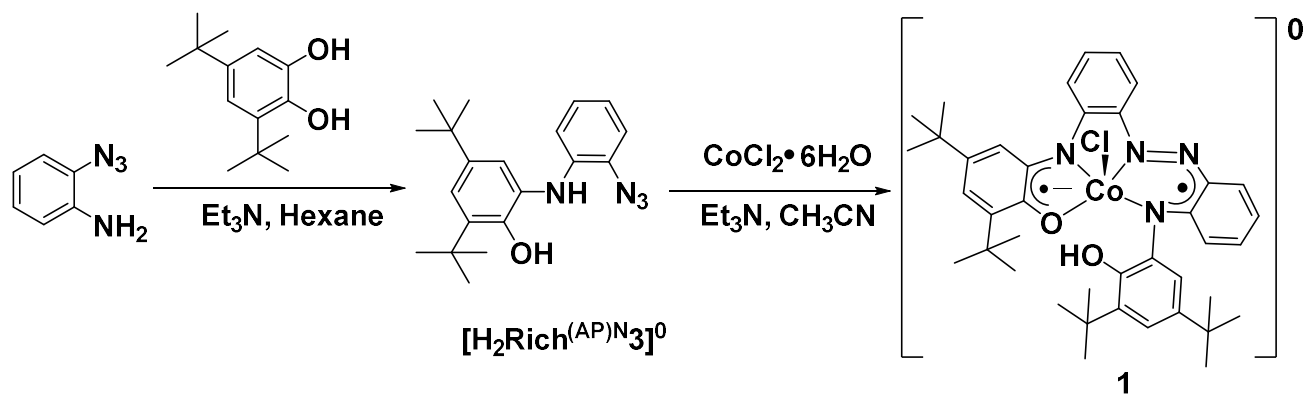
1.9487	615	0.0287	α -H-2[~89%L] → α -L[~94%L](22%) α -H-1[~96%L] → α -L[~94%L](29%) β -H-1[~90%L] → β -L+1[~94%L](24%)	CT (amidophenolate ring → azo and amido phenyl ring) and minor MLCT (metal → azo) CT (phenoxyazine-ring → azo and amido phenyl ring) CT (amidophenolate ring → azo and amido phenyl ring)
2.5897	463	0.1319	β -H-7[~85%L] → β -L[~98%L](24%) β -H-6[~81%L] → β -L[~98%L](58%)	MLCT (metal → phenoxyazine-ring) CT (amidophenolate ring → phenoxyazine-ring) and MLCT (metal → phenoxyazine-ring)
3.1188	384	0.1116	α -H-1[~96%L] → α -L+2[~99%L](46%)	π to π^* transition

^aH and L stands for KS-HOMO and KS-LUMO, respectively.

^bCT and MLCT stands for charge transfer and metal-to-ligand chanrge transfer, respectively.

Scheme S1

Reference 32 in the text: Chandan Mukherjee and co-workers: *Dalton Trans.*, 2015, **44**, 3724–3727.



- ✓ Co(II) (3d series) complex.
- ✓ Six-membered chelate ring holds a dangling phenol.
- ✓ Phenol ring is out of plane.
- ✓ No intraligand cyclization (phenoxyazine ring formation) in the presence of Et₃N under air.